Living Polymerization of (*o*-(Trimethylsilyl)phenyl)acetylene by Molybdenum Imido Alkylidene Complexes

Richard R. Schrock,* Shifang Luo, Jesse C. Lee, Jr., Nadia C. Zanetti, and William M. Davis

Contribution from the Department of Chemistry 6-331, Massachusetts Institute of Technology, Cambridge, Massachusetts 02139

Received December 11, 1995[⊗]

Abstract: *syn*-Mo(CHCMe$_2$Ph)(NAd)[OCH(CF$_3$)$_2$]$_2$(2,4-lutidine) (**2a**; Ad = 1-adamantyl) is a distorted trigonal bipyramid in which 2,4-lutidine occupies an axial position, a structure that results from addition of 2,4-lutidine to the CNO face of unstable pseudotetrahedral *syn*-Mo(CHCMe$_2$Ph)(NAd)[OCH(CF$_3$)$_2$]$_2$. **2a** reacts with (*o*-(trimethylsilyl)phenyl)acetylene (*o*-TMSPA) solely via formation of an α-substituted metallacyclobutene intermediate (α addition) that opens to give a single rotamer of a disubstituted alkylidene complex. *o*-TMSPA is smoothly polymerized at a rate $k_{\mathbf{2a}}[\mathbf{2a}]_0[o\text{-TMSPA}]$ when [**2a**] < 1 mM with a propagation rate constant $k_{\mathbf{2a}} = 0.30\ s^{-1}\ M^{-1}$. Additional studies confirmed that the disubstituted alkylidene propagating species is essentially base-free ($K_{\mathbf{2a}} = 62\ M^{-1}$) and that the propagating species is stable under catalytic conditions (25 °C). Other versions of the Mo(CHCMe$_2$Ph)(NAd)[OCH(CF$_3$)$_2$]$_2$(base) catalyst are either inactive (base = pyridine) or unstable (base = 2-(3-pentyl)pyridine). Mo(CHCMe$_2$Ph)(NAr′)(OC$_6$F$_5$)$_2$(quinuclidine) (**7**; Ar′ = 2,6-Me$_2$C$_6$H$_3$) will also react smoothly with (*o*-(trimethylsilyl)phenyl)acetylene to give poly(*o*-TMSPA) with $K_7 = 1380\ M^{-1}$ and $k_7 = 0.23\ s^{-1}\ M^{-1}$. Low-polydispersity polyenes containing up to 150 equiv of *o*-TMSPA can be obtained readily using either catalyst. The thermodynamically most stable form of poly(*o*-TMSPA), which contains ∼25 double bonds, is air-sensitive and has a significantly red-shifted λ_{max}. *o-t*-BuPA also can be polymerized to give highly conjugated polyenes, but *o-i*-PrPA, *o*-MePA, and phenylacetylene itself add to initiator **2a** with decreasing α regiospecificity (73%, 60%, and 56%, respectively). A lack of regiospecificity we propose leads to polymers that do not have a pure head-to-tail structure, have a lower degree of conjugation, and have a progressively more blue-shifted λ_{max}.

Introduction

Organic polymers that contain a π conjugated backbone have significant potential as nonlinear optical (NLO) materials.[1−5] Among the advantages that such materials might have over inorganic crystals that display similar NLO properties are a subpicosecond response time and the ability to be subtly "tuned" by systematically varying organic groups within the material. Although polyenes fall into this category of potentially interesting NLO materials, several fundamental problems have prevented establishment of the necessary relationship between chain length, chain structure, and degree of conjugation, with an NLO property such as the third-order molecular hyperpolarizability, γ. One problem is the fact that an unsubstituted polyene that contains more than ∼15 double bonds tends to be insoluble.[6] Polyacetylene itself is a black, intractable, air-sensitive solid that remains relatively poorly characterized at a molecular level. Although polyenes can be prepared by polymerization of disubstituted acetylenes,[7−9] the resulting polymers are not highly conjugated. Polyenes prepared from monosubstituted acetylenes also tend to be poorly conjugated in general and relatively poorly characterized at a molecular level. But an overwhelming problem is the paucity of *living* polymerization systems that would lead to polyenes with a narrow molecular weight distribution about a known number average molecular weight (low polydispersity). Soluble substituted polyenes have been prepared indirectly by ring opening substituted cyclooctatetraenes, but the polydispersities of these polyenes were not consistent with a living polymerization.[10]

There has been significant progress in understanding the principles of alkyne polymerization in the last few years. For example, there is now good evidence that alkynes can be polymerized in a living manner via alkylidene complexes,[11−19] and polyenes prepared from certain substituted phenylacetylenes, in particular (*o*-(trimethylsilyl)phenyl)acetylene (*o*-TMSPA),

[⊗] Abstract published in *Advance ACS Abstracts,* April 15, 1996.

(1) Lytel, R.; Lipscomb, G. F.; Thackara, J.; Altman, J.; Elizondo, P.; Stiller, M.; Sullivan, B. In *Nonlinear Optical and Electroactive Polymers*; Prasad, P. N., Ulrich, D. R., Eds.; Plenum Press: New York, 1987; p 415.

(2) Kobayashi, T.; Hattori, T.; Terasaki, A.; Kurokawa, K. In *Nonlinear Optical and Electroactive Polymers*; Prasad, P. N., Ulrich, D. R., Eds.; Plenum Press: New York, 1987; p 137.

(3) Zyss, J.; Chemla, D. S. In *Nonlinear Optical Properties of Organic Molecules and Crystals*; Chemla, D. S., Zyss, J., Eds.; Academic Press: Orlando, FL, 1987; Vol. 1, p 23.

(4) Prasad, P. N. *Polymer* **1991**, *32*, 1746.

(5) Prasad, P. N.; Williams, D. J. In *Introduction to Nonlinear Optical Effects in Molecules and Polymers*; John Wiley and Sons, Inc.: New York, 1991; p 132.

(6) Knoll, K.; Schrock, R. R. *J. Am. Chem. Soc.* **1989**, *111*, 7989.

(7) Masuda, T.; Tachimori, H. *J. Macromol. Sci., Pure Appl. Chem.* **1994**, *A31*, 1675.

(8) Masuda, T.; Higashimura, T. *Adv. Polym. Sci.* **1986**, *81*, 122.

(9) Masuda, T.; Higashimura, T. *Acc. Chem. Res.* **1984**, *17*, 51.

(10) Gorman, C. B.; Ginsburg, E. J.; Grubbs, R. H. *J. Am. Chem. Soc.* **1993**, *115*, 1397.

(11) Masuda, T.; Fujimori, J. I.; Abrahman, M. Z.; Higashimura, T. *Polym. J.* **1993**, *25*, 535.

(12) Wallace, K. C.; Liu, A. H.; Davis, W. M.; Schrock, R. R. *Organometallics* **1989**, *8*, 644.

(13) Schlund, R.; Schrock, R. R.; Crowe, W. E. *J. Am. Chem. Soc.* **1989**, *111*, 8004.

(14) Fox, H. H.; Schrock, R. R. *Organometallics* **1992**, *11*, 2763.

(15) Makio, H.; Masuda, T.; Higashimura, T. *Polymer* **1993**, *34*, 2218.

(16) Fox, H. H.; Wolf, M. O.; O'Dell, R.; Lin, B. L.; Schrock, R. R.; Wrighton, M. S. *J. Am. Chem. Soc.* **1994**, *116*, 2827.

(17) Mizumoto, T.; Masuda, T.; Higashimura, T. *J. Polym. Sci., Part A: Polym. Chem.* **1993**, *31*, 2555.

(18) Masuda, T.; Mishima, K.; Fujimori, J.; Nishida, M.; Muramatsu, H.; Higashimura, T. *Macromolecules* **1992**, *25*, 1401.

(19) Masuda, T.; Yoshida, T.; Makio, H.; Rahman, M. Z. A.; Higashimura, T. *J. Chem. Soc., Chem. Commun.* **1991**, 503.

0002-7863/96/1518-3883$12.00/0

have been found to be soluble and highly conjugated.[8,9,11,20,21] Significant progress also has been made in the synthesis of a wide variety of molybdenum alkylidene complexes of the type Mo(NR)(CHR′)(OR″)$_2$ (and sometimes Mo(NR)(CHR′)(OR″)$_2$(L), where L is a donor ligand),[22] and to some extent their tungsten relatives,[23,24] and their use as olefin metathesis catalysts. One of the most interesting applications so far is their use as initiators for the living polymerization of strained cyclic olefins such as norbornenes and substituted norbornadienes.[25−28] Therefore a study of the polymerization of *o*-TMSPA by a well-defined alkylidene initiator seemed appropriate, especially in view of the paucity of hard data concerning the mechanism of polymerization of terminal alkynes and the paucity of polyenes prepared by a living polymerization method. We hoped that head-to-tail low-polydispersity poly(*o*-TMSPA) could be prepared, that absolute molecular weights could be determined, and that ultimately we could begin to address questions concerning the correlation of γ with chain length and structure. It should be noted that the synthesis of soluble polyenes containing up to 200 double bonds by the living cyclopolymerization of diethyl dipropargylmalonate[16] has allowed the observation that γ/N, where N is the number of double bonds, begins to maximize at approximately 50 double bonds in this particular polymer.[29] Therefore an important goal is to prepare other types of polyenes that contain greater than 15 double bonds and that have a PDI (M_w/M_n) low enough to be useful for NLO studies.

Investigations into the possibility of polymerizing *o*-TMSPA by well-defined complexes initially focused on pseudo-four-coordinate molybdenum complexes of the type Mo(NAr)(CHR)(OR″)$_2$ (e.g., Ar = 2,6-diisopropylphenyl).[30] Such species are stable toward bimolecular decomposition by virtue of the bulky nature of the Ar group, R (usually CMe_3 or CMe_2Ph initially), and OR″ (e.g., hexafluoro-*tert*-butoxide).[22] At the time, we believed that β addition of the terminal alkyne (eq 1b) would be most desirable, as the bulky R′ group thereby would interact minimally with the bulky ligands in the coordination sphere. We assumed that for Mo in a crowded coordination sphere the intermediate molybdacyclobutene would be relatively unstable compared to the "open" tautomer, the vinyl-substituted alkylidene.[22] Also, we felt that the terminal alkylidene ligand that would result from rearrangement of the molybdacyclobutene intermediate would be inherently more reactive than the disubstituted alkylidene that would result from α addition (eq 1a). (It should be noted at this point that, strictly speaking, the narrowest molecular weight distribution would be possible only if α and β addition pathways were of equal rate or if either α or β addition took place exclusively.[31]) However, initial studies showed that all initiators known in our labs at that time did *not* yield low-polydispersity poly(*o*-TMSPA).[30] We then realized that α addition could be favored if steric interaction between the growing polymer chain (P) and a bulky R′ group were severe, and if the metal were less crowded than normal in complexes of this type. If our initial assumption that a disubstituted alkylidene would be unreactive were also incorrect, then it might be possible to polymerize a terminal alkyne via α addition. This strategy led to the development of initiators that contain relatively "small" alkoxides, which we report here. A portion of this work has appeared in the form of a preliminary communication.[32]

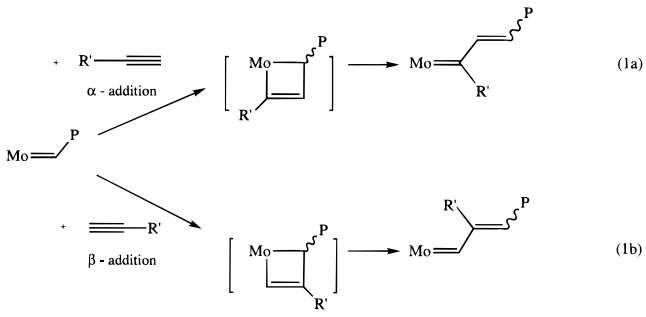

Results

Synthesis and Characterization of Hexafluoroisopropoxide Complexes. Addition of 3 equiv of LiOCH(CF$_3$)$_2$ to Mo(NAd)(CHCMe$_2$Ph)(OTf)$_2$(DME)[33] in diethyl ether yielded the off-white, crystalline, pentane-soluble "ate" complex, Li(DME)Mo(NAd)(CHCMe$_2$Ph)[OCH(CF$_3$)$_2$]$_3$ (**1a**; eq 2). The

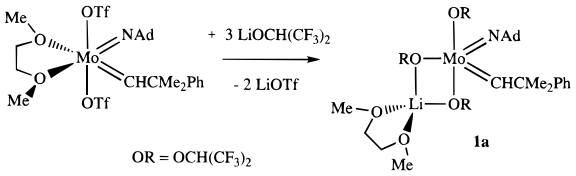

(2)

reaction is relatively complex if less than 3 equiv of LiOCH(CF$_3$)$_2$ is employed, most likely because Mo(NAd)(CHCMe$_2$Ph)[OCH(CF$_3$)$_2$]$_2$ is unstable. (No isolable pseudo-four-coordinate complex of this general type is known in which the alkoxides are not relatively bulky, e.g., *tert*-butoxide, 2,6-disubstituted phenoxides, etc.,[22] and high-oxidation-state alkylidene complexes are known in several cases to decompose bimolecularly by alkylidene coupling to give the olefin.[22]) Proton and carbon NMR spectra of **1a** show the neophylidene H$_\alpha$ resonance at 12.59 ppm and the C$_\alpha$ resonance at 297.9 (J_{CH} = 119 Hz) ppm, respectively. The relatively small value for J_{CH} suggests that the neophylidene ligand is *syn*, i.e., the CMe$_2$Ph group points toward the nitrogen atom of the adamantyl imido ligand. There is no evidence for an H$_\alpha$ resonance in an analogous *anti* complex, which typically is found ∼1 ppm downfield of H$_\alpha$ in the *syn* complex and has a value for J_{CH} of 130−150 Hz.[31] The proton NMR spectrum of **1a** at room temperature also shows three resonances at 6.11, 4.21, and 3.87 ppm for the methine protons in three inequivalent hexafluoroisopropoxide ligands.

(20) Masuda, T.; Hasegawa, K.; Higashimura, T. *Macromolecules* **1974**, *7*, 728.
(21) Masuda, T.; Sasaki, N.; Higashimura, T. *Macromolecules* **1975**, *8*, 717.
(22) Feldman, J.; Schrock, R. R. *Prog. Inorg. Chem.* **1991**, *39*, 1.
(23) Schrock, R. R.; DePue, R. T.; Feldman, J.; Yap, K. B.; Yang, D. C.; Davis, W. M.; Park, L. Y.; DiMare, M.; Schofield, M.; Anhaus, J.; Walborsky, E.; Evitt, E.; Krüger, C.; Betz, P. *Organometallics* **1990**, *9*, 2262.
(24) Wu, Z.; Wheeler, D. R.; Grubbs, R. H. *J. Am. Chem. Soc.* **1992**, *114*, 146.
(25) Schrock, R. R. *Acc. Chem. Res.* **1990**, *23*, 158.
(26) Schrock, R. R. In *Ring-Opening Polymerization*; Brunelle, D. J., Ed.; Hanser: Munich, 1993; p 129.
(27) Novak, B. M.; Risse, W.; Grubbs, R. H. In *Polymer Synthesis Oxidation Processes*; Springer-Verlag: Berlin, 1992; Vol. 102, p 47.
(28) Grubbs, R. H.; Tumas, W. *Science* **1989**, *243*, 907.
(29) Samuel, I. D. W.; Ledoux, I.; Dhenaut, C.; Zyss, J.; Fox, H. H.; Schrock, R. R.; Silbey, R. J. *Science* **1994**, *265*, 1070.
(30) Fox, H. H. Ph.D. Thesis, Massachusetts Institute of Technology, 1993.
(31) Oskam, J. H.; Schrock, R. R. *J. Am. Chem. Soc.* **1993**, *115*, 11831.
(32) Schrock, R. R.; Luo, S.; Zanetti, N.; Fox, H. H. *Organometallics* **1994**, *13*, 3396.
(33) Oskam, J. H.; Fox, H. H.; Yap, K. B.; McConville, D. H.; O'Dell, R.; Lichtenstein, B. J.; Schrock, R. R. *J. Organomet. Chem.* **1993**, *459*, 185.

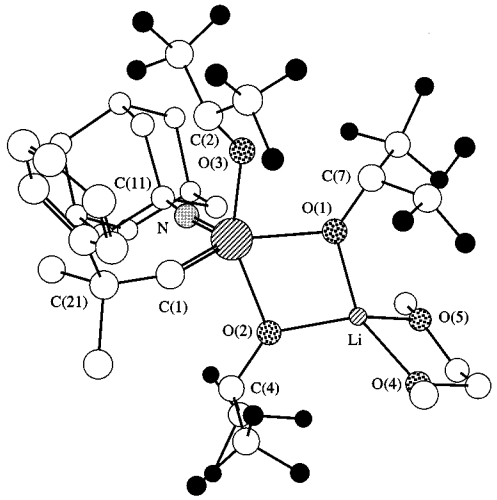

Figure 1. Chem 3D view of the structure of Mo(NAd)(CHCMe$_2$Ph)-[OCH(CF$_3$)$_2$]$_3$Li(MeOCH$_2$CH$_2$OMe) (**1a**).

Table 1. Selected Bond Distances and Angles in **1a**

Distances (Å)					
Mo−C(1)	1.87(2)	Mo−O(2)	2.115(9)	Li−O(2)	1.87(3)
Mo−N	1.67(1)	Mo−O(3)	2.00(2)	Li−O(4)	1.95(3)
Mo−O(1)	2.11(1)	Li−O(1)	1.92(2)	Li−O(5)	1.98(3)
Angles (deg)					
Mo−C(1)−C(21)	152(2)	C(1)−Mo−O(1)	136.2(7)		
Mo−N−C(11)	165(1)	C(1)−Mo−O(2)	92.6(6)		
N−Mo−C(1)	103.3(8)	C(1)−Mo−O(3)	97.3(8)		
N−Mo−O(1)	120.3(6)	O(1)−Mo−O(2)	72.8(4)		
N−Mo−O(2)	105.7(5)	O(1)−Mo−O(3)	80.8(4)		
N−Mo−O(3)	99.1(6)	O(2)−Mo−O(3)	150.3(4)		
O(1)−Li−O(2)	83(1)	O(4)−Li−O(5)	82(1)		
Mo−O(3)−C(2)	136(1)	Mo−O(2)−C(4)	124.3(8)		
Mo−O(1)−C(7)	127.4(8)				

The structure of **1a** was established by X-ray crystallography. (A drawing can be found in Figure 1 and selected bond distances in Table 1). The structure is not of high quality (see supporting information), so bond distances and angles are not known to a high degree of accuracy. The coordination geometry around Mo can be described as either a distorted trigonal bipyramid or a square pyramid. In the trigonal bipyramid description, the two axial ligands are OCH(CF$_3$)$_2$ groups containing O(2) and O(3), while the adamantylimido nitrogen atom, the neophylidene α carbon atom (C(1)), and the oxygen of the third OCH(CF$_3$)$_2$ group (O(1)) lie in the equatorial plane. The sum of the bond angles in the equatorial plane is 360°. The CMe$_2$Ph group points toward the nitrogen atom of the adamantylimido group, as suspected on the basis of NMR data. The Mo═N distance in **1a** is 1.67(1) Å, 0.1 Å shorter than the Mo═N distance (1.767 Å) in *syn*-Mo(CHCMe$_3$)(N-2,6-C$_6$H$_3$-*i*-Pr$_2$)[OCMe(CF$_3$)$_2$]$_2$-(PMe$_3$).[34] The short Mo═N distance in **1a** may be attributed to the better electron-donating ability of the adamantyl group than the (2,6-diisopropylphenyl)imido group and the presence of three electron-withdrawing OCH(CF$_3$)$_2$ groups; both are likely to lead to stronger σ and π bonds in the M−N pseudo triple bond. The Mo═C(1) distance (1.87(2) Å) and the Mo═C(1)−C(2) angle (152°) are normal.[22] Two OCH(CF$_3$)$_2$ groups (one in the equatorial plane, the other one in the axial position) are bridging to the lithium atom. Two bridging OCH(CF$_3$)$_2$ groups and one CH$_3$OCH$_2$CH$_2$OCH$_3$ (DME) produce a distorted tetrahedral geometry about lithium.

When 3 equiv of KOCH(CF$_3$)$_2$ is added to Mo(NAd)(CHCMe$_2$-Ph)(OTf)$_2$(DME), K(DME)$_2$Mo(NAd)(CHCMe$_3$Ph)[OCH(CF$_3$)$_2$]$_3$ is isolated initially. This compound loses 1 equiv of DME under dynamic vacuum to afford what we presume to be the "ate" complex, K(DME)Mo(NAd)(CHCMe$_3$Ph)[OCH(CF$_3$)$_2$]$_3$ (**1b**). **1b** could only be isolated as a yellow oil. Its proton and carbon NMR spectra are analogous to those of **1a**, including an H$_\alpha$ resonance at 12.51 ppm and a C$_\alpha$ resonance at 296.6 ppm (J_{CH} = 119 Hz). The proton NMR spectrum of **1b** at 25 °C in C$_6$D$_6$ only shows two resonances for hexafluoroisopropoxide ligands at 4.07 ppm (two alkoxides) and 6.20 ppm (one alkoxide). We assume that the structure of **1b** is analogous to that of **1a** and that two of the alkoxide methine resonances cannot be resolved from one another in the proton NMR spectrum.

Addition of 1 equiv of boron trifluoride etherate to a cold (−40 °C) solution of **1b** in a 2:1 mixture of ether and pentane produced a white precipitate and a yellow solution. After 2,4-lutidine was added and the white precipitate (which is assumed to be KBF$_3$[OCH(CF$_3$)$_2$]) was filtered off, off-white crystalline Mo(NAd)(CHCMe$_2$Ph)[OCH(CF$_3$)$_2$]$_2$(2,4-lutidine) (**2a**; eq 3) could be isolated. All attempts to isolate "Mo(NAd)(CH-CMe$_2$Ph)[OCH(CF$_3$)$_2$]$_2$" by adding boron trifluoride etherate to **1b** have failed. Evidence presented later suggests that Mo-(NAd)(CHCMe$_2$Ph)[OCH(CF$_3$)$_2$]$_2$ decomposes readily, even in dilute solution (<1 mM). Compound **2a** is prepared most conveniently simply by reacting Mo(NAd)(CHCMe$_2$Ph)(OTf)$_2$-(DME) with 2 equiv of KOCH(CF$_3$)$_2$ in the presence of 2 equiv of 2,4-lutidine. Proton and carbon NMR spectra of **2a** (Table 3) show the neophylidene H$_\alpha$ resonance at 13.76 ppm and the C$_\alpha$ resonance at 297.8 ppm (J_{CH} = 121 Hz), consistent with a *syn* orientation of the neophylidene ligand. In the presence of 1 equiv of 2,4-lutidine at room temperature, resonances for both free and bound 2,4-lutidine are observed, consistent with slow exchange on the NMR time scale between free and bound 2,4-lutidine. **2a** (1−10 mM) reacts rapidly with benzaldehyde to yield PhMe$_2$CH═CHPh (97% *trans*) quantitatively.

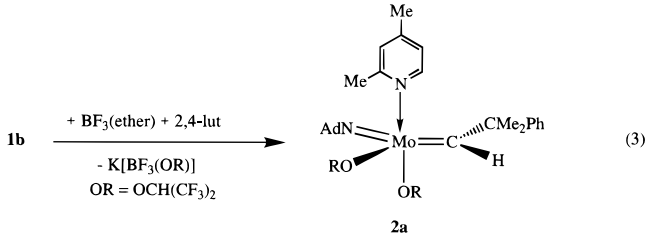

Table 2. Selected Bond Distances and Angles in **2a**

Distances (Å)			
Mo−C(6)	1.880(4)	Mo−O(1)	2.024(3)
Mo−N(1)	1.729(3)	Mo−O(2)	2.012(3)
Mo−N(2)	2.254(3)	N(1)−C(18)	1.450(5)
Angles (deg)			
Mo−C(6)−C(7)	145.5(3)	N(1)−Mo−O(1)	99.8(1)
Mo−N(1)−C(18)	166.1(3)	N(1)−Mo−O(2)	145.5(1)
C(6)−Mo−O(1)	100.7(1)	N(1)−Mo−N(2)	90.9(1)
C(6)−Mo−O(2)	110.7(2)	N(2)−Mo−O(1)	159.2(1)
C(6)−Mo−N(1)	102.9(2)	N(2)−Mo−O(2)	79.1(1)
C(6)−Mo−N(2)	94.2(1)	O(1)−Mo−O(2)	82.0(1)
Mo−O(1)−C(17)	131.4(3)	Mo−O(2)−C(14)	130.2(3)

The results of an X-ray crystallographic study of **2a** are shown in Figure 2 and Table 2. The coordination geometry around Mo in **2a** is similar to what it is in **1a**. In the trigonal bipyramidal description the 2,4-lutidine ligand (N(2)) and one OCH(CF$_3$)$_2$ group (O(1)) occupy the two "axial" positions with an N(2)−Mo−O(1) angle of 159.2°, while N(1), C(6), and O(2) lie in the equatorial plane. (The sum of the three angles in the equatorial plane is 359°.) The neophylidene ligand is *syn*, as

(34) Schrock, R. R.; Crowe, W. E.; Bazan, G. C.; DiMare, M.; O'Regan, M. B.; Schofield, M. H. *Organometallics* **1991**, *10*, 1832.

Table 3. Selected ^{1}H and ^{13}C NMR Data of New Compounds[a]

compound	rotamer	δ (H_α)	δ (C_α)	J_{CH}
Li(DME)Mo(NAd)(CHCMe$_2$Ph)(OR)$_3$ (**1a**)	*syn*	12.59	297.9	119
K(DME)Mo(NAd)(CHCMe$_2$Ph)(OR)$_3$ (**1b**)	*syn*	12.51	296.6	119
Mo(NAd)(CHCMe$_2$Ph)(OR)$_2$(2,4-Me$_2$Py) (**2a**)	*syn*	13.76	297.8	121
Mo(NAd)(CHCMe$_2$Ph)(OR)$_2$(Py) (**2b**)	*syn*	13.76	301.3	121
	anti	14.08		
Mo(NAd)(CHCMe$_2$Ph)(OR)$_2$[2-(3-pentyl)NC$_5$H$_4$] (**2c**)	*syn*	13.76	296.7	121
Mo(NAd)(CHCMe$_2$Ph)(OR)$_2$(Quin) (**2d**)	*syn*	12.81		119
Mo(NAd)[C(Ph-*o*-TMS)(CHCHCMe$_2$Ph)(OR′)$_2$ (**3a/b**)			283.6	
Mo(NAd)(CMePh)(OR)$_2$(2,4-Me$_2$Py) (**5a**)			302.4	
Mo(NAd)(CPh$_2$)(OR)$_2$(2,4-Me$_2$Py) (**5b**)			310.0	
Mo(NAd)[C(Ph)C(Ph)CHCMe$_2$Ph)(OR)$_2$(2,4-Lut) (**6**)			305.1	
Mo(N-2,6-C$_6$H$_4$Me$_2$)(CHCMe$_2$Ph)(OC$_6$F$_5$)$_2$(Quin) (**7a**)	*syn*	13.02		115
	anti	14.16		145
Mo(N-2,6-C$_6$H$_4$-i-Pr$_2$)(CHCMe$_2$Ph)(OR)$_2$(2,4-Lut) (**8**)	*syn*	13.80	295.9	127

[a] Ad = 1-adamantyl; OR = OCH(CF$_3$)$_2$, OR′ = OCMe(CF$_3$)$_2$; Quin = quinuclidine; 2,4-Lut = 2,4-dimethylpyridine.

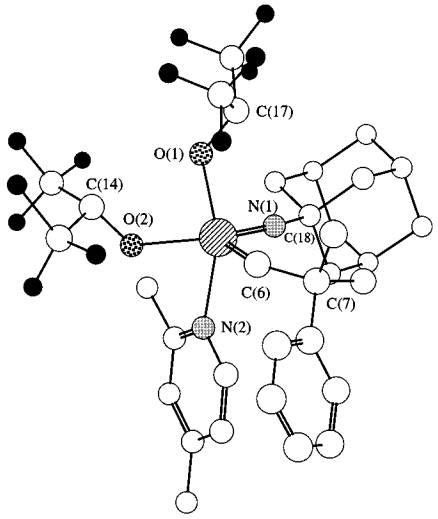

Figure 2. Chem 3D view of the structure of Mo(NAd)(CHCMe$_2$Ph)-[OCH(CF$_3$)$_2$]$_2$(2,4-lutidine) (**2a**).

predicted on the basis of NMR data. The Mo═N distance in **2a** (1.729 Å) is longer than it is in **1a**, but the Mo—C(6) distance (1.880(4) Å) is approximately the same. The equatorial N(1)—Mo—O(2) angle in **2a** (145.5°) is larger than that (120°) in **1a**, possibly because of steric interaction between the *o*-Me group in the 2,4-lutidine ligand and the equatorial AdN and OCH-(CF$_3$)$_2$ groups. Such an interaction would help account for the lability of the 2,4-lutidine in **2a** (see below).

A closer examination of proton NMR spectra of dilute solutions (~0.05−1 mM) of **2a** revealed that some free 2,4-lutidine is always present (~20%, depending on the concentration of **2a**), and that some weak resonances could be observed in the alkylidene region and elsewhere. For some time we entertained the idea that observation of free lutidine was indicative of an equilibrium between **2a** and Mo(NAd)-(CHCMe$_2$Ph)[OCH(CF$_3$)$_2$]$_2$ and therefore that K_1 (k_1/k_{-1} in eq 4) could be measured directly. (An equilibrium constant as large

$$\text{Mo(NAd)(CHCMe}_2\text{Ph)[OCH(CF}_3)_2]_2 + \text{lutidine} \underset{k_{-1}}{\overset{k_1}{\rightleftharpoons}} \mathbf{2a} \quad (4)$$

as 10^5 or 10^6 could be measured by high-field NMR at concentrations below ~1 mM.) We finally came to the conclusion that loss of 2,4-lutidine from **2a** does yield Mo-(NAd)(CHCMe$_2$Ph)[OCH(CF$_3$)$_2$]$_2$ rapidly on the chemical time scale, but that even in dilute solution Mo(NAd)(CHCMe$_2$Ph)-[OCH(CF$_3$)$_2$]$_2$ decomposes readily. The liberated base then stabilizes the remaining **2a** (usually ~80% of the amount added) against further decomposition. Irradiation of the resonance for the proton in the 3-position of ~1 equiv of added 2,4-lutidine (at ~6.5 ppm) did not alter the resonance for H_3 in coordinated lutidine in **2a** (at ~6.1 ppm).

Base adducts analogous to **2a**, Mo(NAd)(CHCMe$_2$Ph)[OCH-(CF$_3$)$_2$]$_2$(L) (L = Py (**2b**), 2-(3-pentyl)NC$_5$H$_4$ (**2c**), or quinuclidine (**2d**)), also could be prepared by methods analogous to that employed for preparing **2a**. An attempt to synthesize an adduct containing 2,6-lutidine yielded decomposition products only, presumably because this base is too bulky to bind strongly to Mo(NAd)(CHCMe$_2$Ph)[OCH(CF$_3$)$_2$]$_2$. It is also clear that 2,4-lutidine in **2a** is readily replaced by a smaller base. For example, addition of 1 equiv of pyridine to a benzene-d_6 solution of **2a** yielded Mo(NAd)(CHCMe$_2$Ph)[OCH(CF$_3$)$_2$]$_2$(Py) (**2b**) immediately, along with resonances characteristic of free 2,4-lutidine. Compounds **2b** and **2d** are stable both in solution and as a solid, while **2c** is stable in solution for only a short time, decomposing to a significant extent after 24 h in solution. **2c** also was found to have decomposed to a significant degree in the solid state after 2 weeks at −40 °C under dinitrogen. We attribute the instability of **2c** to the lability of 2-(3-pentyl)-pyridine and the instability of Mo(NAd)(CHCMe$_2$Ph)[OCH-(CF$_3$)$_2$]$_2$.

NMR data for compounds **2b**−**d** are listed in Table 3. Adducts **2c** and **2d** exist as *syn* rotamers according to the small values for J_{CH}, while **2b** is a 9:1 mixture of *syn* and *anti* rotamers in solution. Only at temperatures below −20 °C do the ^{1}H and ^{13}C NMR spectra for **2c** show sharp alkylidene proton and carbon resonances. At temperatures above −20 °C, all resonances in the ^{1}H NMR spectrum of **2c** are broad, consistent with the relatively rapid exchange of bound 2-(3-pentyl)pyridine in **2c** with free 2-(3-pentyl)pyridine, most likely via formation of Mo(NAd)(CHCMe$_2$Ph)[OCH(CF$_3$)$_2$]$_2$.

Reactions between Alkylidene Complexes and *o*-TMSPA. Compounds **1a**, **1b**, and **2b** do not react readily with *o*-TMSPA, but **2a**, **2c**, and **2d** do. The product of the reaction of *o*-TMSPA with **2a** is only that arising from α addition (eq 1a), as is readily determined from the presence of two olefinic resonances at 8.80 and 4.90 ppm for H_β and H_γ, respectively,[34] in the first insertion product (eq 5). (The product of β addition would be a terminal

$$\mathbf{2a} + o\text{-TMSC}_6\text{H}_4\text{C}{\equiv}\text{CH} \xrightarrow{\text{- lut}} (\text{RO})_2(\text{NAd})\text{Mo}{=}\underset{\text{H}_\beta}{\overset{\text{C}_6\text{H}_4\text{-}o\text{-TMS}}{\text{C}}}{-}\underset{\text{CMe}_2\text{Ph}}{\overset{\text{H}_\gamma}{\text{C}}} \quad (5)$$

OR = OCH(CF$_3$)$_2$

alkylidene with an H_α resonance in the usual region.) The C═C bond in the vinyl group is *trans*, according to the value for $J_{H\beta H\gamma}$ (~16 Hz). Only 3 equiv of *o*-TMSPA is required to consume

Table 4. GPC Data for Poly(*o*-TMSPA) Prepared Employing **2a**

equiv	M_n[a]	PDI	equiv	M_n[a]	PDI
10	1 410	1.07	60	8 810	1.04
20	2 680	1.07	70	9 940	1.05
30	4 400	1.05	80	11 650	1.05
40	5 750	1.05	90	12 500	1.04
50	6 930	1.06	100	13 900	1.04

[a] By GPC versus polystyrene standards.

2a. Interestingly, the first α addition product (the disubstituted alkylidene) does not appear to bind 2,4-lutidine to any significant degree, since 2,4-lutidine resonances are observed essentially where they are found in free 2,4-lutidine, not shifted toward where they are found in the lutidine bound in **2a**. This proposal is corroborated by kinetic studies described later. The bulkier disubstituted alkylidene must block coordination of 2,4-lutidine and also stabilize the four-coordinate complex against decomposition.

Addition of excess *o*-TMSPA to **2a** in either THF or toluene leads to formation of poly(*o*-TMSPA). Polymerization rates in THF are approximately half the rates in toluene under the same experimental conditions, and poly(*o*-TMSPA) prepared in THF generally had a higher PDI (1.10−1.50) compared to that prepared in toluene (PDI = 1.04−1.07). Therefore, in all subsequent polymerizations we employed toluene as the solvent. Table 4 lists the number average molecular weight (by GPC versus polystyrene) of poly(*o*-TMSPA) samples prepared in toluene using initiator **2a**. In initial studies benzaldehyde was added as the "quenching" agent, and the polymer was precipitated with methanol, collected, and dried in vacuo. (In ring opening metathesis polymerization reactions employing initiators of the type described here and norbornadienes or norbornenes as the monomers, benzaldehyde is typically employed to cap the polymer in a Wittig-like reaction with the alkylidene.[26]) The polymers were obtained in >85% yields. A plot of the number average molecular weights (M_n) vs N (the number of equivalents of monomer added) shows a linear relationship (Figure 3), consistent with a living polymerization. Polymers prepared simply by precipitation with methanol were essentially identical to those isolated from reactions that had been quenched with benzaldehyde.

Evidence for quenching of the propagating alkylidene can be obtained indirectly by NMR by observing consumption of *o*-TMSPA. Consumption of *o*-TMSPA ceases ∼20 min after addition of ∼100 equiv of benzaldehyde at ∼20 °C, presumably as a consequence of conversion of propagating alkylidene complexes to analogous oxo species via a Wittig-like reaction. If only a few equivalents of benzaldehyde is added, then at the low concentrations of the catalyst in a typical polymerization reaction, the capping reaction could be incomplete, even after several hours. These results contrast with the rapid reaction of **2a** with benzaldehyde, but are consistent with what we suspect to be a much lower reactivity of a disubstituted alkylidene in general (i.e., toward benzaldehyde or *o*-TMSPA).

An alternative method of quenching polymerization is to add 8 equiv of acetic acid. The amount of Mo in a reprecipitated poly(*o*-TMSPA)$_{20}$ sample was found to be only 14% of the amount of catalyst **2a** that had been employed by elemental analysis for Mo. Therefore in some studies polymerizations were terminated by addition of 8 equiv of degassed acetic acid to the reaction solution and stirring of the mixture at room temperature for 24 h. The polymers obtained after exposure to acetic acid for 24 h in the absence of oxygen had UV/vis spectra that were similar to those of samples that had been allowed to isomerize thermally in the absence of oxygen, as discussed in more detail in a later section.

Initiator **2c** also reacts with *o*-TMSPA via solely α addition and initiates the relatively fast polymerization of *o*-TMSPA in toluene at room temperature compared to the rate of polymerization by initiator **2a**. However, a 45-mer obtained after 3 h of polymerization time shows a bimodal molecular weight distribution by GPC with M_n = 565 200 (PDI = 1.06) and M_n = 20 020 (PDI = 1.07), respectively, for the two peaks (by viscometry; theory = 7960 absolute molecular weight). Since the predictable propagating species must be the same type as shown in eq 5, the faster polymerization initiated by **2c** can be attributed to formation of higher molecular weight polymer by some more active polymerization catalyst. When the same polymerization reaction was run for 23 h the M_n values of the two distributions were found to be 387 200 (PDI = 1.27) and 17 250 (PDI = 1.09), respectively. When more than 1 equiv of 2,4-lutidine was added to a toluene solution of **2c** before addition of 40 equiv of *o*-TMSPA, a polymer having a unimodal molecular weight distribution and low PDI was formed (M_n = 17 000 by viscometry; PDI = 1.08). We also do not observe bimodal molecular weight distributions and polymer degradation in reactions employing **2a** as the initiator in toluene. We conclude that 2,4-lutidine prevents some decomposition that produces a more active catalyst or "poisons" a more active polymerization catalyst that is formed under the reaction conditions. A more active catalyst could arise through decomposition of a fraction of **2c** (as a consequence of the high lability of the base in **2c**) or through reactions of **2c** with impurities or water. A small amount of relatively active catalyst would lead to the formation of high molecular weight polymer and secondary metathesis (chain degradation). Evidently the decomposition product or products that are formed when **2a** is employed as an initiator are likewise "deactivated" by 2,4-lutidine and do not further complicate polymerizations.

The rate of polymerization of *o*-TMSPA by initiator **2a** could be followed by proton NMR, although we found gas chromatography to be more accurate and reliable. Plots of $\ln(C/C_0)$ versus time (after initiator was consumed) in the presence of 80 equiv of *o*-TMSPA were found to be linear through more than 3 half-lives, and the observed rate was found to depend to the first power upon the total initiator present ($[\mathbf{2a}]_0$). (See Table 9a for individual values.) If we assume that the rate of loss of base from a base adduct ($k_{-2}[\mathrm{Cat}_n(\mathrm{B})]$; eq 6) is larger than $k_{\mathbf{2a}}[\mathrm{Cat}_n][\mathrm{M}]$ (M = monomer) (eq 7), and $[\mathrm{Cat}_n] \approx [\mathbf{2a}]_0$, the rate of disappearance of monomer is approximately equal to $k_{\mathbf{2a}}[\mathbf{2a}]_0[\mathrm{M}]$. From 13 runs (Table 9a) we get a value of $k_{\mathbf{2a}}$ =

$$\mathrm{Cat}_n + \mathrm{B} \underset{k_{-2}}{\overset{k_2}{\rightleftharpoons}} \mathrm{Cat}_n(\mathrm{B}) \qquad (6)$$

$$\mathrm{Cat}_n + \mathrm{M} \xrightarrow{k_{\mathbf{2a}}} \mathrm{Cat}_{n+1} \qquad (7)$$

0.30 with a range of 0.24−0.36 s^{-1} M^{-1} (Table 5). Other assumptions are the following: (i) the reaction of M with Cat_n is irreversible; (ii) the reactivities of Cat_n and Cat_{n+1} alkylidene intermediates are identical; and (iii) there is only one mechanism or mode of chain growth. (The possible involvement of rotamers will be considered later.)

When a significant amount of base (B = 2,4-lutidine) is added (10−75 equiv) the rate of disappearance of *o*-TMSPA is again found to be cleanly first order, but the rate in the presence of ∼75 equiv of added base slows to ∼25% of its "base-free" value. If we make the same assumptions as we did above, then the rate is that shown in eq 8 (where $K_{\mathbf{2a}} = k_2/k_{-2}$). Therefore a plot of $[\mathbf{2a}]_0/k_{\mathrm{obs}}$ versus [2,4-lutidine] ([B]) should produce a

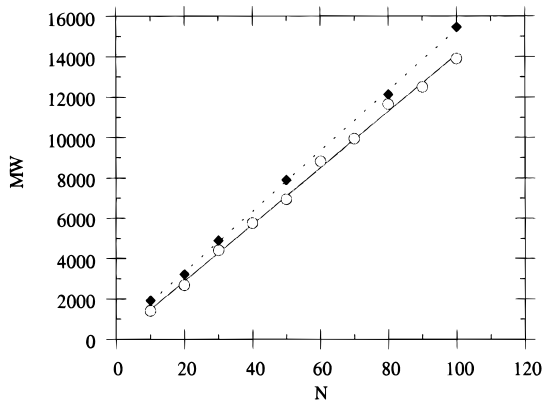

Figure 3. Plot of molecular weight (by GPC vs polystyrene) for poly(*o*-TMSPA) prepared from *N* equiv of *o*-TMSPA and **2a** (○) or **7** (◆) as the initiator in toluene.

Table 5. Summary of Observed Rate and Equilibrium Constants[a]

constant	value	no. of expts	range
k_{2a}	0.30 s^{-1} M^{-1}	13	0.24−0.36
K_{2a}	62 M^{-1}	5	(see Figure 4a)
K_{2d}	2810 M^{-1}	1	
$k_{3b\rightarrow 3a}$	3.1×10^{-4} s^{-1}	2	3.01, 3.19
k_{3a}	1.2×10^{-3} s^{-1} M^{-1}	1	
k_{3b}	6.3×10^{-3} s^{-1} M^{-1}	1	
k_7	0.23 s^{-1} M^{-1}	4	(see Figure 4b)
K_7	1380 M^{-1}	4	(see Figure 4b)

[a] See Experimental Section for individual values.

straight line with intercept $1/k_{2a}$ and slope K_{2a}/k_{2a} (eq 9). From

$$\frac{d[M]}{dt} = -\frac{k_{2a}[\mathbf{2a}]_0[M]}{1 + K_{2a}[B]} = -k_{obs}[M] \quad (8)$$

$$\frac{[\mathbf{2a}]_0}{k_{obs}} = \frac{1}{k_{2a}} + \frac{K_{2a}}{k_{2a}}[B] \quad (9)$$

5 runs (see Table 9b for data and details) we obtained a value of $k_{2a} = 0.32$ s^{-1} M^{-1} and $K_{2a} = 62$ M^{-1} (Figure 4a). These results are consistent with our initial assumptions above, since if $K_{2a} = 62$ M^{-1}, then at a $[\mathbf{2a}]_0$ of 1 mM ∼95% of the metal is in the base-free form. Therefore $K_{2a}[B] \ll 1$ in the absence of added base and the rate of disappearance of monomer equals $k_{2a}[\mathbf{2a}]_0[M]$. In the presence of 17 equiv of added base, for example ($[\mathbf{2a}]_0 = 10^{-3}$ M), $K_{2a}[B]$ is ∼1 and the rate is approximately halved.

We can now estimate a value for k_{-2} (at $[\mathbf{2a}]_0 = 10^{-3}$ M and [M] = 0.08 M) since we know that $k_{-2}[Cat_n(B)]$ should be at least 10 times $k_{2a}[Cat_n][M]$. In order for this to be true, k_{-2} must be ∼5 s^{-1} or greater. Resonances are broad in the room temperature proton and carbon spectra of **2c**, a result that suggests that the rate of loss of 2-(3-pentyl)pyridine from **2c** is approaching the NMR time scale (50−100 s^{-1}). Loss of 2-(3-pentyl)pyridine from **2c** should be faster than loss of 2,4-lutidine from **2a** for steric reasons, so k_{-2} should be much less than 50−100 s^{-1}. Therefore a value for k_{-2} of ∼5 s^{-1} would seem to be approximately correct.

It would be useful to determine the rate at which M reacts with "Mo(NAd)(CHCMe$_2$Ph)[OCH(CF$_3$)$_2$]$_2$", formed when **2a** loses 2,4-lutidine, in order to compare it with the rate of propagation. Unfortunately, the consumption of **2a** is simply too fast at 25 °C to measure using NMR techniques under pseudo-first-order conditions; for example, initiation is complete in 1−2 min when [M] ≈ [B] ≈ 1 M. Since we cannot determine

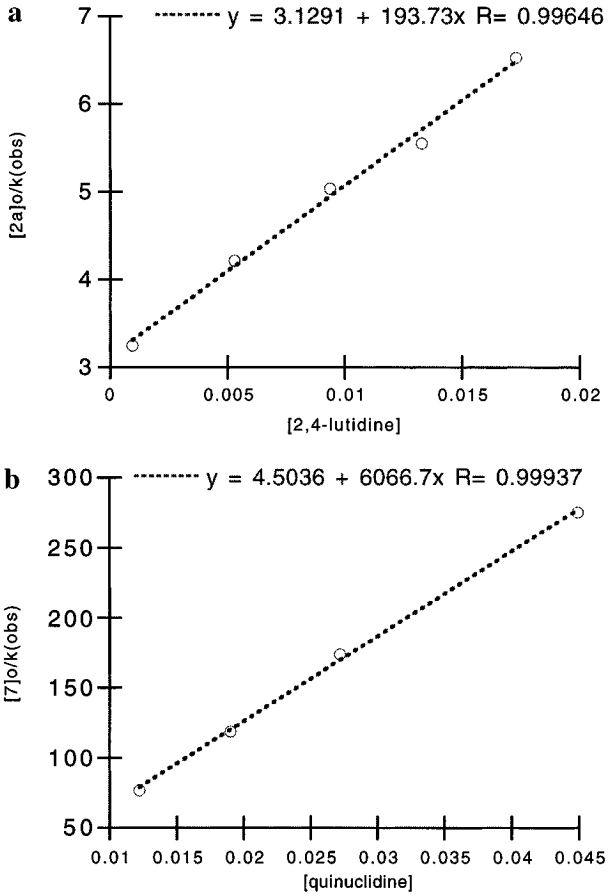

Figure 4. (a) Plot of $[\mathbf{2a}]_0/k_{obs}$ versus [2,4-lutidine] for polymerization of *o*-TMSPA; determination of k_{2a} and K_{2a}. (b) Plot of $[\mathbf{7}]_0/k_{obs}$ versus [quinuclidine] for polymerization of *o*-TMSPA; determination of k_7 and K_7.

K_1 (the equilibrium constant for binding 2,4-lutidine to the initiator), we cannot determine k_i.

Compound **2d** polymerizes *o*-TMSPA in a manner analogous to that of **2a**. Since the rate constant for propagation (k_{2a}) is known, K_{2d} can be measured as a consequence of a single rate measurement using eq 9. K_{2d} was found to be 2810 M^{-1}. The larger value for K_{2d} versus K_{2a} (62 M^{-1}) is consistent with the greater basicity of quinuclidine versus 2,4-lutidine in forming adducts of this type. K_{2d} is also approximately twice the size of the binding constant in the case of Mo(N-2,6-Me$_2$C$_6$H$_3$)(CHCMe$_2$Ph)(OC$_6$F$_5$)$_2$(quinuclidine) (see later).

Isolation of a "First Insertion Product" and Observation of a "Second Insertion Product" in the Reaction between Mo(NAd)(CHCMe$_2$Ph)[OCMe(CF$_3$)$_2$]$_2$ and *o*-TMSPA. Although the "first insertion product" of the reaction of **2a** with *o*-TMSPA could be observed by proton NMR, all attempts to isolate it failed, probably because it reacts with additional *o*-TMSPA too readily to give mixtures of oligomers. However, addition of 1 equiv of *o*-TMSPA to Mo(NAd)(CHCMe$_2$Ph)[OCMe(CF$_3$)$_2$]$_2$[33] in pentane at −40 °C leads to a mixture of *two* "first insertion products" (**3a** and **3b**) in a variable ratio (usually approximately 9:1) in favor of **3a**. Proton NMR spectra of the mixture contain two sets of doublets, one set at 7.34 and 5.78 ppm ($J_{HH} = 15.6$ Hz, $\Delta = 1.56$ ppm between resonances) for **3a**, and the other set at 8.44 and 4.30 ppm ($J_{HH} = 15.6$ Hz, $\Delta = 4.14$ ppm between resonances) for **3b**. The J_{HH} values are consistent with a *trans* C=C bond in each compound. When *o*-TMS(C$_6$H$_4$)C≡CD was employed, the resonances at 7.34 (**3a**) and 8.44 (**3b**) were absent, indicating that the acetylene proton from *o*-TMSPA is found in the β position in the disubstituted

vinylalkylidene ligand, as expected. Carbon NMR spectra of the **3a**/**3b** mixture contain a resonance at 283.6 ppm for the alkylidene carbon of the major product (**3a**), but the alkylidene resonance for **3b** could not be observed with certainty as a consequence of its concentration being too low. In **3a** the resonances for C_β and C_γ are at found at 126.3 (J_{CH} = 150 Hz) and 122.8 ppm (J_{CH} = 150 Hz), respectively, consistent with the proposal that this species is a vinyl-substituted alkylidene complex.[13,34] We propose that **3a** and **3b** are the two rotamers shown in eq 10.

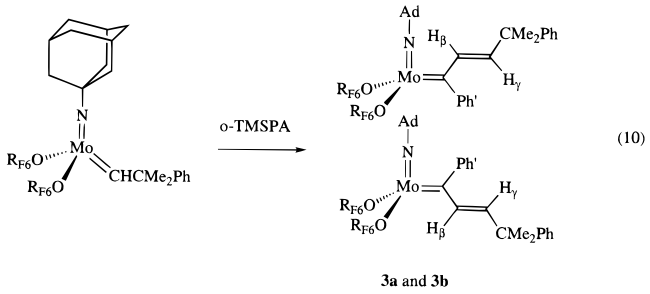

3a and **3b** (10)

The mixture of **3a** and **3b** can be isolated in ∼60% yield as deep red microcrystals. NMR spectra of the isolated material are identical in all respects to spectra observed upon treating Mo(NAd)(CHCMe$_2$Ph)[OCMe(CF$_3$)$_2$]$_2$ with *o*-TMSPA. However, we noticed that the ratio of **3a** to **3b** depended upon the history of the sample and changed with time to an equilibrium value of 5−7 at 24 °C in favor of **3a**. When the reaction time is shortened to 5 min, and the reaction solution is kept below ∼0 °C during workup, the product is an approximately 1:1 mixture of **3a** and **3b**. In solvents such as C_6D_6 and over a period of ∼1 day at room temperature, the 1:1 mixture returned to the equilibrium value. The conversion of **3b** to equilibrium was found to be first order with values at 24 °C of $k_{\mathbf{3b}\rightarrow\mathbf{3a}}$ = 3.01 × 10^{-4} s^{-1} and $K_{\mathbf{3b}\rightarrow\mathbf{3a}}$ = 7.3.

The rotamer proposal is supported by the fact that irradiation of the **3a**/**3b** mixture with a medium-pressure mercury lamp at −60 °C increases the amount of **3b** to approximately 25% of the total after 24−48 h, a phenomenon that has been observed for rotamers of other alkylidene complexes in this general class.[31] The rate at which equilibrium was reestablished was followed at 15 °C and found to be first order through 3 half-lives with $k_{\mathbf{3b}\rightarrow\mathbf{3a}}$ = 1.05 × 10^{-4} s^{-1} ($K_{\mathbf{3b}\rightarrow\mathbf{3a}}$ = 6.3 at 15 °C). At 24 °C $k_{\mathbf{3b}\rightarrow\mathbf{3a}}$ = 3.19 × 10^{-4} s^{-1} ($K_{\mathbf{3b}\rightarrow\mathbf{3a}}$ = 5.5), in agreement with the result quoted above. These rate constants should be compared to that for conversion of the disfavored *anti* rotamer of Mo(NAd)(CHCMe$_2$Ph)[OCMe(CF$_3$)$_2$]$_2$ to the *syn* rotamer in toluene at −31.4 °C (5.75 × 10^{-4} s^{-1}).[31] At 15 °C the latter should be of the order of ∼10^{-2} s^{-1}; i.e., the rate of conversion of rotamers of **3b** to **3a** is approximately 2 orders of magnitude slower. It is important to note that the reaction between *o*-TMSPA and **2a** yields only one first insertion product, with olefinic resonances at 4.90 and 8.80 ppm (Δ = 3.90 ppm), chemical shifts and a Δ value that would make it most analogous to the *minor* product (**3b**) in the **3a**/**3b** mixture (4.50 and 8.44 ppm, Δ = 4.14 ppm). The other rotamer of the first insertion product of **2a** probably is not formed readily, unless the rotamer isomerization rate is extremely fast. This seems unlikely in view of the slow rate of rotamer isomerization in the OCMe(CF$_3$)$_2$ system. Therefore we can have some confidence that *only one rotamer is formed in each insertion step* in the polymerization of *o*-TMSPA by **2a** and that the chain grows in only one way. It is not clear which rotamer is which in either the OCH(CF$_3$)$_2$ or the OCMe(CF$_3$)$_2$ system. However, the bulkier OCMe(CF$_3$)$_2$ ligands appear to destabilize the sterically more favorable conformation found in the OCH(CF$_3$)$_2$ system. The OCMe(CF$_3$)$_2$ system would clearly be the more crowded, in general, whichever rotamer is considered. We assume that greater steric hindrance in general in the OCMe(CF$_3$)$_2$ system is what prevents the ready polymerization of *o*-TMSPA at 25 °C.

A mixture of **3a** and **3b** reacts slowly with 1 equiv of *o*-TMSPA to yield two "second insertion" products, as indicated by olefinic doublets in the proton NMR spectrum at 5.99 and 5.23 ppm (J_{HH} = 15.6 Hz) along with a singlet at 8.87 ppm, and a second set of doublets at 6.11 and 5.27 ppm (J_{HH} = 15.6 Hz) along with a singlet at 8.12 ppm. When the mixture was heated to 70 °C, the intensities of the resonances ascribed to the two second insertion products increased at the expense of those for **3a** and **3b**. It is proposed that the second insertion products are also a mixture of two rotamers in solution (eq 11).

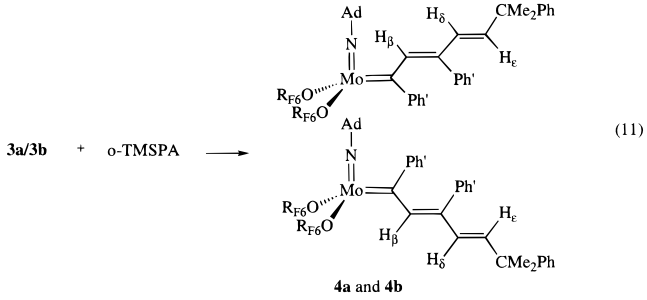

4a and **4b** (11)

The singlet resonances at 8.87 and 8.12 ppm are assigned the H_β protons, while the doublets are ascribed to the H_δ and H_ϵ protons. The rate of disappearance of **3a** and **3b** at 23 °C was found (by NMR) to be first order in the presence of ∼25 equiv of *o*-TMSPA. The *major* rotamer reacted with a rate constant $k_{\mathbf{3a}}$ = 1.2 × 10^{-3} s^{-1} M^{-1} (R^2 = 0.995) while for the minor rotamer $k_{\mathbf{3b}}$ = 6.3 × 10^{-3} s^{-1} M^{-1} (R^2 = 0.983). The value for $k_{\mathbf{3b}}$ can be compared with the value for $k_{\mathbf{2a}}$ in the catalytic reaction initiated by **2a** ($k_{\mathbf{2a}}$ = 0.30 s^{-1} M^{-1}). The rate of reaction of what appear to be analogous rotamers with *o*-TMSPA in the OCH(CF$_3$)$_2$ system (**2a**) is ∼50 times faster than in the OCMe(CF$_3$)$_2$ system, a clear demonstration of the relative steric influence of OCH(CF$_3$)$_2$ versus OCMe(CF$_3$)$_2$.

Synthesis of Other Initiators Containing OCH(CF$_3$)$_2$ Ligands. Two disubstituted alkylidene complexes, Mo(NAd)(CMePh)[OCH(CF$_3$)$_2$]$_2$(2,4-lutidine) (**5a**) and Mo(NAd)(CPh$_2$)[OCH(CF$_3$)$_2$]$_2$(2,4-lutidine) (**5b**), could be synthesized by treating **2a** with α-methylstyrene or 1,1′-diphenylethylene, respectively (eq 12). Both **5a** and **5b** are bright yellow microcrystalline solids that are soluble in benzene, toluene, and ether and slightly soluble in pentane. The ^{13}C chemical shift values for the disubstituted alkylidene carbon atom are 302 ppm for **5a** and 310 ppm for **5b** (see also Table 3). Only a single rotamer is observed for **5a**.

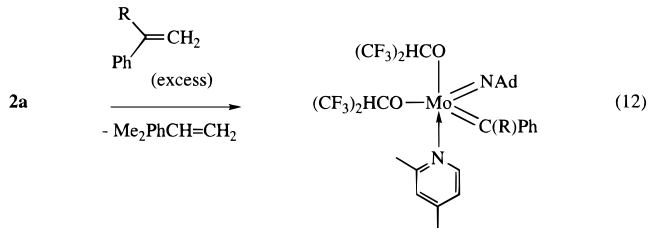

R = Me (**5a**), Ph (**5b**) (12)

Diphenylacetylene reacts with **2a** to give an isolable "first insertion product", Mo(NAd)[C(Ph)C(Ph)CHCMe$_2$Ph][OCH(CF$_3$)$_2$]$_2$(2,4-lutidine) (**6**) as a single rotamer. The ^{13}C chemical shift value for the disubstituted alkylidene carbon atom is 305

Table 6. Results of Initiation Reactions between **2a** and *o*-$RC_6H_4C{\equiv}CH$ (R = H, Me, *i*-Pr, *t*-Bu)

initiator	R	α (%)	*β* (%)
2a	*t*-Bu	100	
2a	*i*-Pr	73	27
2a	Me	60	40
2a	H	56	44

ppm (see also Table 3). More diphenylacetylene does not react readily with **6** at 25 °C.

Proton NMR studies in benzene-d_6 show that *o*-TMSPA reacts with **5a**, **5b**, and **6** solely via α addition, and all three compounds serve as initiators for the polymerization of *o*-TMSPA in toluene. Poly(*o*-TMSPA)$_{150}$ prepared with initiator **5a** had PDI = 1.08; poly(*o*-TMSPA)$_{40}$ prepared with initiator **5b** had PDI = 1.04; and poly(*o*-TMSPA)$_{80}$ prepared with initiator **6** had PDI = 1.12. These results lend further support to the proposal that disubstituted (vinyl) alkylidenes are the reactive intermediates in the polymerization of *o*-TMSPA by **2a**.

Reactions between Alkylidene Complexes and Other Ortho-Substituted Phenylacetylenes (R = H, Me, *i*-Pr, *t*-Bu). Table 6 lists the results of reactions between **2a** and *o*-$RC_6H_4C{\equiv}CH$ (R = H, Me, *i*-Pr, *t*-Bu). Addition of only 2 equiv of *o*-*t*-BuPA is necessary in order to consume all **2a**. Phenylacetylenes that contain progressively smaller ortho substituents react with **2a** to give progressively more *β* addition in the first step. If we assume that all alkynes react in fundamentally the same way, most likely at the CNO face of the pseudo-four-coordinate initiator,[26] we can attribute an increasing amount of *β* addition to a decreased steric interaction between the neophylidene ligand and the ortho-substituted phenyl ring.

The "smaller" phenylacetylenes also react with disubstituted alkylidenes by both α and *β* addition to varying degrees. Both *o*-*t*-BuPA and *o*-TMSPA add to the Mo=CMePh bond in **5a** 100% via α addition. However, *o*-MePA and *o*-*i*-PrPA react with **5a** by both α and *β* addition, with the amount of *β* addition being ~7% of the total initial concentration of **5a** in each case. (The actual ratio of α vs *β* first insertion products could not be determined because of the complexity of the proton NMR spectra.) Similar studies employing **6** show that *o*-MePA, *o*-*i*-PrPA and *o*-TMSPA all add to the Mo=C(Ph)C(Ph)CHCMe$_2$Ph bond 100% via α addition, but phenylacetylene itself reacts via both α (90%) and *β* addition. The steric demands of the disubstituted alkylidene ligand in **6** clearly cause α insertion to be much more favored. The above data suggest that during polymerization of *o*-*i*-PrPA, *o*-MePA, and especially phenylacetylene itself, *some β* addition of the monomer to one or both rotamers of the propagating Mo=C(*o*-RC_6H_4)(P) species is likely. Therefore there is a significant possibility that these polyenes are not completely regular (head to tail), at least when prepared by the $OCH(CF_3)_2$ catalysts, and that the regiospecificity declines as the size of the R group in the ortho position decreases.

Compound **2a** serves as an initiator for the polymerization of *o*-MePA and *o*-*i*-PrPA under conditions used for the polymerization of *o*-TMSPA. Poly(*o*-MePA) and poly(*o*-*i*-PrPA) were isolated as red powders that appear to be analogous to polymers reported in the literature.[7] GPC and UV/vis data for these polymers are presented in Table 7. The PDI values are larger than those for poly(*o*-TMSPA). The polydispersity of poly(*o*-*i*-PrPA) is smaller than that for poly(*o*-MePA), possibly as a consequence of a higher α selectivity in the propagation step, although different rotamers with different reactivities might also be accessible and could contribute to a broadening of the molecular weight distribution. The values for λ_{max} in poly(*o*-*i*-PrPA) and poly(*o*-MePA) are markedly and progressively more blue-shifted in chains of comparable length versus λ_{max} in poly(*o*-TMSPA). For a 100-mer, λ_{max} for poly(*o*-TMSPA) is ~538 nm (see also below), for poly(*o*-*i*-PrPA) it is 456 nm, and for poly(*o*-MePA) it is 444 nm. The marked decrease in λ_{max} could be ascribed to progressively less selective α addition and consequently a less regular structure and less conjugation in the polymer backbone.

Initiators That Contain Other Imido or Alkoxide Ligands. It would be desirable to establish whether initiators that contain other "small alkoxides" can be prepared and whether they also will polymerize *o*-TMSPA smoothly. Another important question is whether the adamantylimido ligand is required. Adamantylimido complexes[33] have not been explored to any significant extent as catalysts for more standard polymerization reactions of norbornenes or substituted norbornadienes, but in the one instance where an adamantylimido catalyst has been explored in some detail, it was found to behave in a significantly different manner than the analogous arylimido catalysts.[31]

Addition of 2 equiv of KOC_6F_5 to Mo(CHCMe$_2$Ph)(NAr′)(triflate)$_2$(1,2-dimethoxyethane) (NAr′ = N-2,6-Me$_2$C$_6$H$_3$) in 1,2-dimethoxyethane followed by 1 equiv of quinuclidine yields a complex with the composition Mo(CHCMe$_2$Ph)(NAr′)(OC$_6$F$_5$)$_2$(quinuclidine) (**7**) as a mixture of *anti* and *syn* isomers having alkylidene proton resonances at 14.16 and 13.02 ppm, respectively. Initially the ratio of *syn* to *anti* was typically 95:5, after several days ~75:25, and after 2 weeks ~55:45. This behavior is analogous to formation of a *syn* rotamer of Mo(NAr)(CH-*t*-Bu)[OCMe(CF$_3$)$_2$]$_2$(PMe$_3$) first and with time the more stable *anti* rotamer (exclusively, in this case, within a few days).[34] Such behavior is indicative of a larger binding constant for a base to the *anti* form than to the *syn* form, and it suggests also a greater inherent reactivity of the *anti* form than the *syn* form toward olefins and acetylenes. (Greater reactivity of Mo(NAr)(CH-*t*-Bu)[OCMe(CF$_3$)$_2$]$_2$ toward several norbornadienes has been confirmed.[31])

When excess *o*-TMSPA is added to a *syn*/*anti* mixture of **7**, a smooth first-order consumption of each initiator can be observed (unlike the rapid consumption of initiator **2a**), but no insertion products were evident (as they were in the case of **2a**). If we assume that loss of quinuclidine from either the *syn* or *anti* form of **7** is fast relative to reaction of Mo(NAd)(CHCMe$_2$Ph)(OCH(CF$_3$)$_2$)$_2$ with *o*-TMSPA, then these data are consistent with a larger binding constant for quinuclidine in **7** compared to 2,4-lutidine in **2a**. The observed rate constant for disappearance of **7**$_{syn}$ under pseudo-first-order conditions was found to be 7.61×10^{-4} s^{-1} ($R^2 = 0.985$), while the observed rate constant for disappearance of **7**$_{anti}$ was found to be 1.13×10^{-4} s^{-1} ($R^2 = 0.930$). A more rapid consumption of **7**$_{syn}$ (by a factor of ~7) is again consistent with the larger binding constant for quinuclidine in **7**$_{anti}$, assuming that *anti*-Mo(CHCMe$_2$Ph)(NAr′)(OC$_6$F$_5$)$_2$ would be the most reactive inherently.

Polymerizations of *o*-TMSPA in toluene using **7** (largely the *syn* rotamer) as an initiator proceed smoothly to give low polydispersity poly(*o*-TMSPA) that is essentially identical to poly(*o*-TMSPA) prepared employing **2a** (Table 4). In this case also the relationship between M_n and the number of equivalents of *o*-TMSPA employed is linear (Figure 3). If we assume that the polymerization of *o*-TMSPA initiated by **7** can be described in a manner similar to the reaction initiated by **2a** (eqs 6 and 7), and that loss of quinuclidine from the propagating species is faster than chain growth, then eqs 13 and 14 (cf. 8 and 9) are valid. (K_7 is the binding constant and k_7 the propagating rate

$$\frac{d[M]}{dt} = -\frac{k_7[\mathbf{7}]_0[M]}{1 + K_7[B]} = -k_{obs}[M] \quad (13)$$

$$\frac{[\mathbf{7}]_0}{k_{obs}} = \frac{1}{k_7} + \frac{K_7}{k_7}[B] \quad (14)$$

constant.) The rate of the consumption of monomer was followed in the presence of 9−33 equiv of quinuclidine (four runs; see Table 10), and the resulting values for $[\mathbf{7}]_0/k_{obs}$ were plotted against the quinuclidine concentration (Figure 4b). From the slope and intercept we obtain the values $k_7 = 0.23\ s^{-1}\ M^{-1}$ and $K_7 = 1380\ M^{-1}$. The value for k_7 is approximately the same as that for $k_{\mathbf{2a}}$, but K_7 is ∼22 times larger than $K_{\mathbf{2a}}$. Therefore at a concentration of 1 mM ∼50% of the quinuclidine is bound to the metal, but in the presence of 30 equiv of added quinuclidine ∼98% of the quinuclidine is bound to the metal, leading to a significantly slower rate of polymerization in the absence of added quinuclidine and a sharp decrease in the rate when quinuclidine is added. Therefore the K_7[B] term in the denominator of eq 13 cannot be ignored at catalyst concentrations of ∼1 mM, even in the absence of added quinuclidine.

Mo(NAr)(CHCMe$_2$Ph)[OCH(CF$_3$)$_2$]$_2$(2,4-lutidine) (**8**) has also been prepared from Mo(CHCMe$_2$Ph)(NAr)(OTf)$_2$(DME), KOCH(CF$_3$)$_2$, and 2,4-lutidine in ether. (Proton and carbon NMR spectral data are listed in Table 3.) Only one rotamer (*syn*; J_{C-H} = 127 Hz) is readily observable at room temperature. Proton NMR spectroscopic studies show that **8** reacts with *o*-TMSPA 100% via α addition. Approximately 3.5 equiv of *o*-TMSPA is required to consume all **8**. We did not observe the first insertion product by proton NMR. Poly(*o*-TMSPA)$_{80}$ prepared with initiator **8** is also a purple solid. However, the GPC trace of the polymer contains two peaks with $M_n = 2.26 \times 10^5$ (PDI = 1.46) and $M_n = 4.47 \times 10^4$ (PDI = 1.14). The bimodal molecular weight distribution in poly(*o*-TMSPA) prepared by catalyst **8** is similar to that observed in poly(*o*-TMSPA) prepared by catalyst **2c**. The origin of the bimodal distribution is unknown, and this initiator was not studied further.

All attempts to prepare a 2,4-lutidine adduct of Mo(NAr′)(CHCMe$_2$Ph)(OC$_6$F$_5$)$_2$ failed, suggesting that 2,4-lutidine does not bind strongly enough to form a stable adduct. These results are consistent with the finding that $K_7 = 1380\ M^{-1}$ while $K_{\mathbf{2d}}$ is approximately twice that (2814 M^{-1}); i.e., the metal binds quinuclidine more strongly when OCH(CF$_3$)$_2$ ligands are present than when OC$_6$F$_5$ ligands are present.

UV/Vis Spectroscopic Properties of Poly(*o*-TMSPA). Samples of poly(*o*-TMSPA) prepared here are initially purple with a single broad absorption centered at 526 nm for the 10-mer out to 538 nm for the 100-mer in their UV−vis spectra (Table 8). If a sample in THF is not exposed to air, the spectrum changes over a period of several days at 22 °C to one that has two absorptions, one shifted significantly to lower energy (600−700 nm) and one shifted to higher energy, as shown for the 10-, 20-, and 30-mers in Figures 5, 6, and 7. The approximate area fraction of the low-energy absorption decreases with chain length, but the λ_{max} for the low-energy absorption increases with chain length to ∼680 nm for the 30-mer. (The location of the low-energy absorption in the long polymers is difficult to determine accurately because the intensity is low.) Upon the exposure of samples in THF to air, the low-energy absorption disappears immediately and λ_{max} for the remaining absorption is approximately 538 nm for the longest polymers. However, the low-energy absorption is least noticeable for the longer polymers. For example, the main absorption in the 100-mer is at 538 nm with a shoulder at 680 nm. With time that shoulder shifts slightly to approximately 700 nm, but the main absorption is still at 538 nm. After exposure to air, only the 538 nm absorption remains. Therefore only samples containing less than 80 equiv of monomer show the red-shifted absorption to a significant degree, and only in the absence of air. The UV−vis spectra of samples that were isolated by treatment with acetic acid in the absence of air are approximately the same as those after several days in solution in the absence of air. The formation of polymers having a low-energy absorption also seems to depend upon solvent. The low-energy absorption is not observed in toluene in the absence of air over a period of several days, although a sample that has been "isomerized" in THF that is then isolated by precipitation with methanol has

Table 7. GPC and UV−Visible Data of Poly(*o*-MePA) and Poly(*o*-*i*-PrPA)

	poly(*o*-MePA)			poly(*o*-i-PrPA)		
equiv	M_n	PDI	λ_{max} (nm)	M_n	PDI	λ_{max} (nm)
20	3 970	1.16	426	4 790	1.09	444
30	4 550	1.17	434	5 990	1.09	450
40	5 760	1.16	436	7 610	1.10	454
60	7 260	1.24	440	11 020	1.15	454
70	8 580	1.30	442	13 700	1.16	456
80	10 160	1.24	442	14 160	1.09	456
90	11 950	1.35	440	14 900	1.09	456
100	13 570	1.25	444	16 320	1.09	456

[a] By GPC versus polystyrene standards.

Table 8. λ_{max} of Poly(*o*-TMSPA)

N	as isolated (no acid)	after 5−6 days	after air
10	526	470, 600	464
20	526, ∼660 (sh)[a]	505, ∼660	512
30	534, ∼660 (sh)	520, ∼670	526
40	534, ∼660 (sh)	534, ∼670 (sh)	530
50	530, ∼660 (sh)	530, ∼670 (sh)	534
60	534, ∼660 (sh)	530, ∼670 (sh)	538
70	538, ∼660 (sh)	536, ∼670 (sh)	534
80	538, ∼660 (sh)	540, ∼700 (sh)	536
90	538, ∼ 680 (sh)	538, ∼700 (sh)	538
100	538, ∼680 (sh)	538, ∼700 (sh)	538

[a] Shoulder.

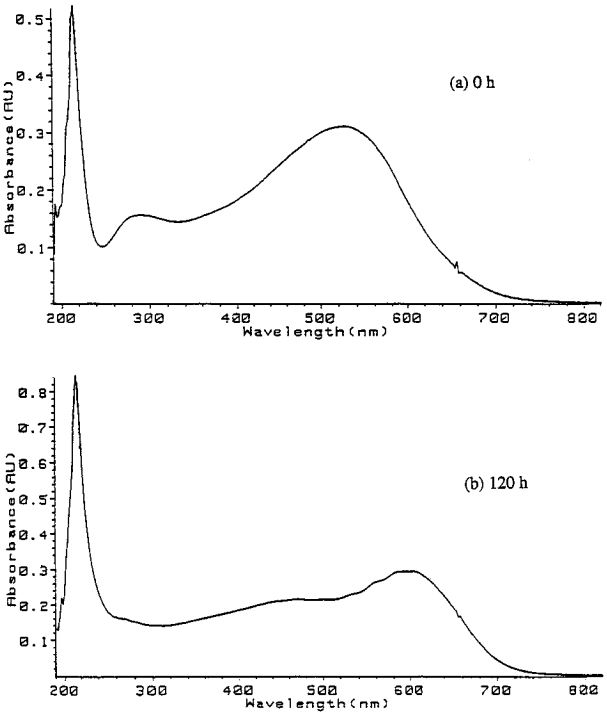

Figure 5. UV−vis spectra of (*o*-TMSPA)$_{10}$ in THF in the absence of air.

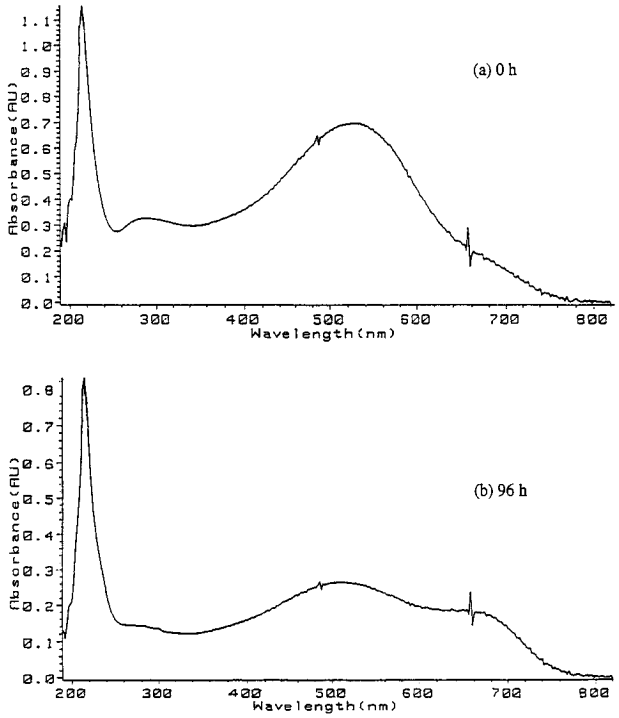

Figure 6. UV−vis spectra of $(o\text{-TMSPA})_{20}$ in THF in the absence of air.

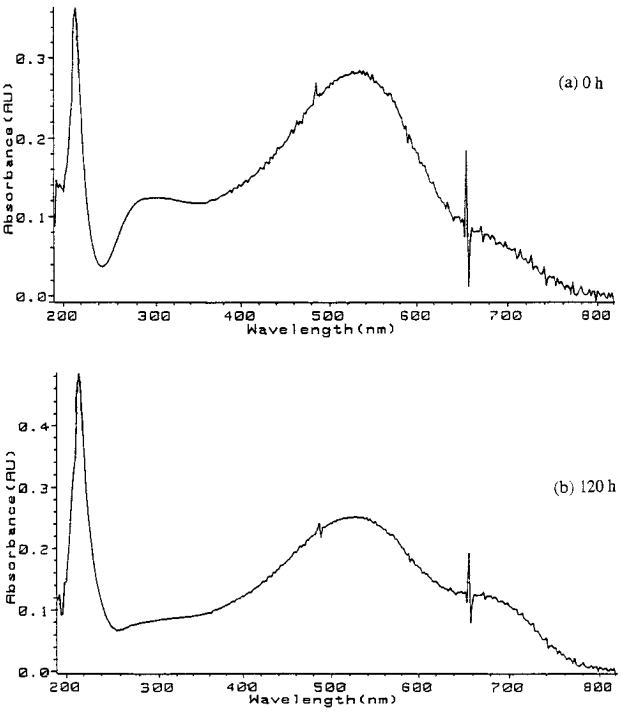

Figure 7. UV−vis spectra of $(o\text{-TMSPA})_{30}$ in THF in the absence of air.

the same spectrum in toluene as it did in THF. The final spectrum appears to be an equilibrium state.

Our working hypothesis is that the low-energy absorption can be ascribed to highly conjugated sequences of poly(*o*-TMSPA), and these sequences are not produced initially in the polymerization reaction. The most plausible explanation is that the highly conjugated form is *all-trans* and that *cis*/*trans* isomerization can take place thermally, or rapidly if catalyzed by acetic acid. The "*all-trans* sequence" can of course involve the entire chain, if the chain length is such that the *all-trans* form is significantly more stable than other forms, and if *cis*/*trans* isomerization is facile. It is difficult to say what the percentage of *all-trans* sequences is since the molar extinction coefficient is likely to be larger for "*trans*" than for "*cis*" forms. It is natural that these "low band gap" "*trans*" polyene sequences will be significantly more air sensitive than "*cis*" polyene sequences. It is important to note that only polyenes containing fewer than approximately 50 equiv are obviously air sensitive and therefore that poly(*o*-TMSPA) prepared with classical catalysts,[7] which has a relatively high molecular weight, would not appear to be air sensitive.

Discussion and Conclusions

One of the most important features of the work described here is that disubstituted alkylidene complexes are the propagating species in a controlled polymerization of *o*-TMSPA and that they form exclusively only when interaction of the *o*-(trimethylsilyl)phenyl group with the coordination sphere around the metal is quantitatively reduced compared to interaction of the *o*-(trimethylsilyl)phenyl group with the disubstituted alkylidene. Disubstituted alkylidenes of the type observed here are significantly less reactive than terminal alkylidenes, but they still react with a terminal acetylene readily at 25 °C. A disubstituted alkylidene complex is also very much more stable than a terminal alkylidene complex toward bimolecular alkylidene coupling reactions and, therefore, possibly could be employed in reactions at higher temperatures, or in the presence of certain functionalities (e.g., a ketone or internal olefin). It seems likely that successful polymerization of *o*-TMSPA by classical alkylidene catalysts[7] also depends on selective α addition of *o*-TMSPA to a disubstituted alkylidene and on the stability of disubstituted alkylidene intermediates in general.

A second noteworthy feature of the results reported here is that base adducts of otherwise unstable alkylidene complexes can be used successfully as initiators. The success of this approach depends upon the special circumstances surrounding polymerization of *o*-TMSPA with initiator **2a** or **7**, namely, that *stable*, *base-free*, *propagating* species are formed, and upon choosing a base that is labile enough to be lost relatively rapidly to give the base-free initiator, but not one that is so weakly bound that catalyst decomposition or side reactions become significant problems during initiator preparation or polymerization reactions. Up to this point we have been concerned largely with designing stable four-coordinate catalysts containing a primary alkylidene and understanding rotamer interconversion and reactivity. The stabilization of an *initiator* by coordination of base that is reported here should be compared to stabilization of a *propagating* species by coordination of base, where the rate of propagation is thereby reduced relative to the rate of initiation.[13,35] Designing appropriate base adducts for a given polymerization reaction will likely become an important aspect of controlled polymerization by well-defined catalysts in the future.

Third, we were surprised to find that polymers prepared from ortho-substituted phenylacetylenes in which the ortho substituent was not TMS or *tert*-butyl are almost certainly not regular head-to-tail polymers, largely because steric repulsion between the propagating disubstituted alkylidene and the ortho-substituted phenyl ring of the incoming alkyne is not significant enough to make the alkyne add α exclusively. At this point we do not know whether such "mistakes" alone are responsible for the lower conjugation of polyenes prepared from "smaller" phenylacetylenes, but that is certainly a good possibility. We cannot comment upon the nature of the poly(phenylacetylenes) made with catalysts that operate by mechanisms other than the

(35) Wu, A.; Grubbs, R. H. *Macromolecules* **1995**, *28*, 3502.

alkylidene mechanism. We hope in the future to be able to prepare other phenylacetylenes that we can confirm are exclusively head-to-tail polymers in order to begin to understand the structure of such polyenes in more detail, how λ_{max} correlates with polyene structure, and the extent to which the ortho substituent controls the structure of exclusively head-to-tail poly(phenylacetylenes).

Finally, it is worth noting that poly(*o*-TMSPA) containing only ~20 monomers (on the average) isomerizes thermally to a significant extent to give (presumably *all-trans*) forms having λ_{max} between 600 and 700 nm. These forms have not been observed for poly(*o*-TMSPA) prepared with classical catalysts,[7] either because the molecular weight of such polymers is generally too high or because such polymers were exposed to air, or both. Isomerization of polyene oligomers (<15 double bonds)[6] or substituted polyenes prepared by ring opening of monosubstituted cyclooctatetraenes[10] to *trans*-rich or *all-trans* forms has been observed. In neither case does the red-shifted form have λ_{max} > 600 nm. At this point it is not known whether the low-band-gap forms of poly(*o*-TMSPA) that we observe here are unique to poly(*o*-TMSPA), or whether they can be observed in other regular head-to-tail polyenes in this general class when ~20 double bonds are present.

The results reported here should be compared with a recent report that catalysts in this family that contain triphenylacetate ligands allow only β addition of the propargylic terminal triple bonds in diethyl dipropargylmalonate and thereby formation of only cyclohexene rings in the polyene backbone formed in a cyclopolymerization reaction.[36] The inherent regiochemical problem associated with addition of a terminal alkyne to an alkylidene would appear to be on its way to being solved to some degree simply by employing "small" alkoxides or "large" carboxylate ligands on the metal.

Experimental Section

All manipulations were performed under a nitrogen atmosphere in a Vacuum Atmosphere drybox or using standard Schlenk techniques. Reagent grade ether and tetrahydrofuran were distilled from sodium benzophenone ketyl under nitrogen. Pentane was washed with 5% nitric acid in sulfuric acid, stored over calcium chloride, and then distilled from sodium benzophenone ketyl under nitrogen. Dichloromethane was distilled from calcium hydride under nitrogen. Toluene was distilled from molten sodium under nitrogen.

All deuterated NMR solvents were passed through a column of activated alumina. NMR data are listed in parts per million downfield from tetramethylsilane for proton and carbon, and relative to $CFCl_3$ for fluorine. Coupling constants are quoted in hertz. Variable temperature NMR spectroscopic studies were recorded without calibrating the probe temperature.

Gel permeation chromatography (GPC) was carried out using Shodex KF-802.5, -803, -804, -805, and -800P columns, a Knauer differential refractometer, and a Viscotek differential refractometer/viscometer H-500 on samples 0.1−0.3% w/v in THF which were filtered through a Millex-SR 0.5 mm filter in order to remove particulates. GPC columns were calibrated versus polystyrene standards (Polymer Laboratories Ltd.) of MW 1206 to 1.03×10^6.

Synthesis of Li(DME)Mo(NAd)(CHCMe$_2$Ph)[OCH(CF$_3$)$_2$]$_3$ (1a). Solid $LiOCH(CF_3)_2$ (150 mg, 0.862 mmol) was added in one portion to a cold ether solution (~10 mL) of Mo(NAd)(CHCMe2Ph)$(OTf)_2$(DME) (225 mg, 0.263 mmol). After the solution was stirred for 2 h at room temperature, the ether was removed from the yellow reaction solution in vacuo. The yellow residue was extracted with pentane (~20 mL), and the extract was filtered through Celite to afford a light yellow solution, from which off-white crystalline **1a** was obtained upon cooling of the solution to −40 °C; yield 190 mg (71%): ^{1}H NMR (C_6D_6) δ 12.59 (s, 1, C*H*CMe$_2$Ph), 7.35 (d, 2, Ph), 7.15 (t, 2, Ph), 7.01 (t, 1, Ph), 6.11 (sept, OC*H*$(CF_3)_2$, J_{FH} = 7.3), 4.21 (sept, OC*H*$(CF_3)_2$, J_{FH} = 6.6), 3.87 (sept, OC*H*$(CF_3)_2$, J_{FH} = 6.2), 2.97 (s, 6, OC*H*$_3$), 2.73 (s, 4, OC*H*$_2$), 2.19 (br, 6, C*H*$_2$), 1.94 (br, 3, C*H*), 1.81 (s, 3, C*Me*$_2$Ph), 1.73 (s, 3, C*Me*$_2$Ph), 1.48 (q, 6, C*H*$_2$); ^{13}C NMR (C_6D_6) δ 297.87 (*C*HCMe$_2$Ph, J_{CH} = 119), 148.61 (C_{ipso}), 129.08 (Ph), 125.92 (Ph), 126.73 (Ph), 84.72 (m, OC*H*$(CF_3)_2$), 83.13 (m, OC*H*$(CF_3)_2$), 71.75 (m, OCH$(CF_3)_2$), 75.59 (AdN), 69.64 (O*C*H$_2$), 58.71 (O*C*H$_3$), 50.60 (*C*Me$_2$Ph), 43.94 (*C*H$_2$, AdN), 36.06 (*C*H$_2$, AdN), 29.99 (*C*H, AdN), 31.97 (C*Me*$_2$Ph), 31.33 (C*Me*$_2$Ph); ^{19}F NMR (C_6D_6) δ 75.71, −75.95, −76.46, −76.64, −76.90. The elemental analysis sample for **1a**, crystals grown in the presence of DME, has the formula Li(DME)$_2$Mo(NAd)(CHCMe$_2$Ph)-[OCH$(CF_3)_2]_3$. Anal. Calcd for $C_{37}H_{50}NF_{18}O_7Mo$: C, 41.98; H, 4.76; N, 1.32. Found: C, 41.79; H, 4.75; N, 1.47.

Synthesis of K(DME)Mo(NAd)(CHCMe$_2$Ph)[OCH(CF$_3$)$_2$]$_3$ (1b). Compound **1b** was prepared as a yellow oil by a method analogous to that described for **1a**: ^{1}H NMR (C_6D_6) δ 12.51 (s, 1, C*H*CMe$_2$Ph), 7.40 (d, 2, Ph), 7.19 (t, 2, Ph), 7.04 (t, 1, Ph), 6.20 (sept, 1, OC*H*$(CF_3)_2$, J_{FH} = 7.2), 4.07 (sept, 2, OC*H*$(CF_3)_2$, J_{FH} = 6.6), 2.84 (s, 6, OC*H*$_3$), 2.79 (s, 4, OC*H*$_2$), 2.21 (d, 6, C*H*$_2$), 1.98 (s, 3, C*H*), 1.83 (s, 6, C*Me*$_2$-Ph), 1.54 (q, 6, C*H*$_2$); ^{13}C NMR (C_6D_6) δ 296.62 (*C*HCMe$_2$Ph, J_{CH} = 119), 149.44 (C_{ipso}), 130.03 (Ph), 125.43 (Ph), 124.98 (Ph), 84.44 (sept, J_{CF} = 29), 73.87 (AdN), 72.33 (sept, J_{CF} = 29), 71.07 (O*C*H$_2$), 58.23 (O*C*H$_3$), 50.04 (*C*Me$_2$Ph), 44.20 (AdN), 36.22 (AdN), 31.93 (AdN), 29.99 (C*Me*$_2$Ph); ^{19}F NMR (C_6D_6) δ −74.38, −75.13, −75.47.

Synthesis of Mo(NAd)(CHCMe$_2$Ph)[OCH(CF$_3$)$_2$]$_2$(2,4-lutidine) (2a). Solid $KOCH(CF_3)_2$ (1.47 g, 7.13 mol) was added to a cold ether (~60 mL) slurry of Mo(NAd)(CHCMe$_2$Ph)$(OTf)_2$(DME) (3.00 g, 3.50 mmol) . One hour later, 2,4-lutidine (0.50 mL, 4.32 mmol) was added. The resulting mixture was stirred at room temperature overnight and then filtered through Celite. Removal of the ether from the filtrate in vacuo afforded a yellow solid. The yellow solid was taken up in ~10 mL of toluene, and the Celite-filtered solution was diluted with ~80 mL of pentane. This solution was stored in a −40 °C freezer overnight to give large off-white crystals of **2a**; yield 2.51 g (88%): ^{1}H NMR (C_6D_6) δ 13.76 (s, 1, C*H*CMe$_2$Ph), 7.56 (d, 1, 2,4-Lut), 7.34 (d, 2, Ph), 7.13 (t, 2, Ph), 7.02 (t, 1, Ph), 6.20 (sept, 1, OC*H*$(CF_3)_2$, J_{FH} = 6.6), 6.12 (s, 1, 2,4-Lut), 5.85 (d, 1, 2,4-Lut), 4.50 (sept, 1, OC*H*$(CF_3)_2$, J_{FH} = 6.0), 2.35 (s, 3, Me$_o$), 1.96 (s, 3, C*Me*$_2$Ph), 1.89 (br, 6, C*H*$_2$), 1.77 (br, 3, C*H*), 1.56 (s, 3, C*Me*$_2$Ph), 1.40 (s, 3, Me$_p$), 1.36 (br, 6, C*H*$_2$); ^{13}C NMR (C_6D_6) δ 297.8 (*C*HCMe$_2$Ph, J_{CH} = 121), 158.5 (Py), 155.8 (Py), 150.8 (Py), 148.1 (C_{ipso}, Ph), 130.0 (Ph), 127.4 (Py), 126.6 (Ph), 126.2 (Ph), 122.4 (Py), 83.4 (sept, OC*H*$(CF_3)_2$, J_{CF} = 30), 75.0 (sept, OC*H*$(CF_3)_2$, J_{CF} = 29), 72.8 (AdN), 50.0 (C*Me*$_2$Ph), 43.8 (AdN), 36.2 (AdN), 32.0 (C*Me*$_2$Ph), 31.0 (C*Me*$_2$Ph), 29.9 (AdN), 26.3 (*Me*, 2,4-Lut), 20.39 (*Me*, 2,4-Lut); ^{19}F NMR (C_6D_6) δ −74.99, −74.63, −74.54. Anal. Calcd for $C_{33}H_{38}N_2O_2F_{12}Mo$: C, 48.42; H, 4.68; N, 3.42. Found: C, 48.11; H, 4.83; N, 3.56.

Synthesis of Mo(NAd)(CHCMe$_2$Ph)[OCH(CF$_3$)$_2$]$_2$(Py) (2b). Compound **2b** was synthesized in 44% yield by the same method as that used to prepare **2a**: ^{1}H NMR (*syn* rotamer, C_6D_6) δ 13.31 (s, 1, C*H*CMe$_2$Ph), 8.35 (d, 2, Py), 6.90−7.10 (m, 5, Py + Ph), 6.60 (m, 1, Ph), 6.25 (m, 3, Py + OC*H*$(CF_3)_2$), 4.37 (sept, 1, OC*H*$(CF_3)_2$, J_{FH} = 6.6), 1.88 (s, 3, C*Me*$_2$Ph), 1.84 (b, 6, C*H*$_2$), 1.78 (b, 3, C*H*), 1.49 (s, 3, C*Me*$_2$Ph), 1.34 (b, 6, C*H*$_2$); ^{13}C NMR (C_6D_6) δ 301.2 (*C*HCMe$_2$Ph, J_{CH} = 121), 152.4 (Py), 147.3 (C_{ipso}, Ph), 138.6 (Py), 128.8 (Ph), 126.4 (Ph), 126.0 (Ph), 124.1 (Py), 84.1 (m, OC*H*$(CF_3)_2$), 75.2 (m, OC*H*-$(CF_3)_2$), 73.4 (AdN), 50.4 (C*Me*$_2$Ph), 43.8 (AdN), 35.8 (AdN), 31.7 (C*Me*$_2$Ph), 30.3 (C*Me*$_2$Ph), 29.5 (AdN); ^{19}F NMR (C_6D_6) δ −68.85, −69.32, −69.66, −70.29.

Synthesis of Mo(NAd)(CHCMe$_2$Ph)[OCH(CF$_3$)$_2$]$_2$(2-(3-pentyl)-NC$_5$H$_4$) (2c). Compound **2c** was prepared in 72% yield by a method analogous to that used to prepare **2a**. The compound decomposes quickly at room temperature and at low temperature (−40 °C) after a long period of time, even in the solid state: ^{1}H NMR ($C_6D_5CD_3$, −35 °C) δ 13.76 (s, 1, C*H*CMe$_2$Ph), 8.46 (d, 1), 7.34 (d, 2, Ph), 7.14 (t, 2, Ph), 7.03 (t, 1, Ph), 6.73 (t, 1), 6.33 (m, 2), 6.12 (m, 1, OC*H*$(CF_3)_2$), 4.21 (m, 1, OC*H*$(CF_3)_2$), 2.24 (m, 1, C*H*Et$_2$), 1.94 (b, 9, CMe$_2$Ph + NAd), 1.82 (br, 3, CH), 1.70 (s, 3, CMe$_2$Ph), 1.40 (m, 6, NAd); ^{13}C NMR (CD_2Cl_2, −35 °C) δ 296.76 (*C*HCMe$_2$Ph, J_{CH} = 121), 164.7 (Py), 149.6 (Py), 148.3 (C_{ipso}, Ph), 139.5 (Py), 128.8 (Ph), 126.6 (Ph), 125.8 (Ph), 123.6 (Py), 120.7 (Py), 83.1 (sept, OC*H*$(CF_3)_2$, J_{CF} = 30), 73.7 (sept, OC*H*$(CF_3)_2$, J_{CF} = 29), 72.9 (AdN), 51.0 (CMe$_2$Ph), 43.0

(36) Schattenmann, F. J.; Schrock, R. R.; Davis, W. M. *J. Am. Chem. Soc.* **1996**, *118*, 3296.

(AdN), 35.8 (AdN), 32.6 (CMe_2Ph), 30.3 (CMe_2Ph), 29.9 ($CHEt_2$), 29.7 (AdN), 28.7 (CH_2CH_3), 27.0 (CH_2CH_3), 11.9 (CH_2CH), 10.4 (CH_2CH_3); ^{19}F NMR (CD_2Cl_2, −35 °C) δ −76.53, 76.78, 77.77. Anal. Calcd for $MoC_{36}H_{44}N_2O_2F_{12}$: C, 50.24; H, 5.15; N, 3.25. Found: C, 50.15; H, 5.55; N, 3.25.

Synthesis of Mo(NAd)(CHCMe$_2$Ph)[OCH(CF$_3$)$_2$]$_2$(quinuclidine) (2d). To a 3 mL solution of 39 mg of **2a** (0.047 mmol) in toluene was added 26 mg of quinuclidine (0.24 mmol) at room temperature. All solvents and excess quinuclidine were removed in vacuo after 1 h, and the solid residue was recrystallized from 1 mL of pentane at −30 °C to give 28 mg of off-white crystalline product (70%): ^1H NMR (C_6D_6) δ 12.81 (s, 1, C*H*CMe$_2$Ph, J_{CH} = 119), 7.02−7.10 (m, 4, Ph), 6.92−6.97 (m, 1, Ph), 6.13 (sept, 1, OC*H*(CF$_3$)$_2$, J_{FH} = 7.1), 4.26 (sept, 1, OC*H*(CF$_3$)$_2$, J_{FH} = 6.3), 2.78 (m, 6, quinuclidine), 2.02 (br, 6, C*H*$_2$), 1.89 (s, 6, CH*Me*$_2$Ph), 1.45 (s, 6, C*H*$_2$), 1.39 (br, 3, C*H*), 1.09 (m, 6, quinuclidine), 0.93 (br, 6, quinuclidine).

Synthesis of Mo(NAd)[C(*o*-TMS-C$_6$H$_4$)(CH═CHCMe$_2$Ph)][OCMe(CF$_3$)$_2$]$_2$ (3a/b). A pentane solution (60 mL) of the compound Mo(NAd)(CHCMe$_2$Ph)[OCMe(CF$_3$)$_2$]$_2$ (1.00 g, 1.35 mmol) was cooled to −40 °C. To the cold yellow solution was added *o*-TMSPA (239 mg, 1.37 mmol). The mixture was then kept cold at −40 °C for $^1/_2$ h. During this period, the mixture assumed a deep red color. The red solution was then filtered through Celite, concentrated in vacuo to ∼10 mL, and put into a −40 °C freezer. Deep red microcrystalline solid was obtained after a few days; yield 658 mg (53%): ^1H NMR (C_6D_6, minor) δ 8.44 (d, H$_\beta$, J = 15.6), 6.9−7.7 (m, H's of Ph's), 4.30 (d, H$_\gamma$, J = 15.6), 0.34 (TMS); ^1H NMR (C_6D_6, major) δ 7.34 (d, H$_\beta$, J = 15.6), 6.9−7.7 (m, H's of Ph's), 5.78 (d, H$_\gamma$, J = 15.6), 0.22 (TMS); ^{13}C NMR (major, C_6D_6) δ 283.6, 1, 126.3 (J_{CH} = 150), 122.8 (J_{CH} = 150). Anal. Calcd for $MoC_{39}H_{47}NO_2F_{12}Si$: C, 51.26; H, 5.18; N, 1.53. Found: C, 51.53; H, 5.52; N, 1.69.

Synthesis of Mo(NAd)(CMePh)[OCH(CF$_3$)$_2$]$_2$(2,4-lutidine) (5a). α-Methylstyrene (0.105 mL, 0.808 mmol) was added to an ether solution of **2a** (578 mg, 0.71 mmol). After 24 h the ether was removed in vacuo to leave a dark yellow oily residue. Recrystallization of the residue from pentane gave **5a** as bright yellow microcrystals; yield 312 mg (56%): ^1H NMR (C_6D_6) δ 8.45 (d, 1, 6, 2,4-Lut), 7.68 (dd, 2, J = 1.2, 8.4, Ph), 7.25 (m, 2, Ph), 7.01 (t , 1, Ph), 6.34 (sept, OC*H*(CF$_3$)$_2$), 6.17 (s, 1, 2,4-Lut), 6.02 (d, 1, 6), 4.51 (sept, 1, 6.3, OC*H*(CF$_3$)$_2$), 2.31 (s, 3, 2,4-Lut), 1.92 (br, 6, AdN), 1.76 (br, 3, AdN), 1.50 (br, 3, 2,4-Lut), 1.34 (br, 6, AdN); ^{13}C NMR (C_6D_6) δ 302.4 (*C*Me$_2$Ph), 160.5 (2,4-Lut), 153.3 (2,4-Lut), 151.1 (Ph), 146.7 (2,4-Lut), 129.2 (Ph), 128.1 (Ph), 126.5 (Ph), 123.3 (2,4-Lut), 83.0 (O*C*H(CF$_3$)$_2$), 74.9, 74.5 (═N*C*), 43.6 (NAd), 36.0 (AdN), 29.7 (AdN), 27.4 (Me), 21.4 (Me); ^{19}F NMR (C_6D_6) δ −78.96 (1), −79.19 (1), −79.29 (1), −79.70 (1). Anal. Calcd for $MoC_{31}H_{34}N_2O_2F_{12}$: C, 47.01; H, 4.33; N, 3.54. Found: C, 47.26; H, 4.44; N, 3.49.

Synthesis of Mo(NAd)(CPh$_2$)[OCH(CF$_3$)$_2$]$_2$(2,4-lutidine) (5b). This compound was prepared in 46% yield by the same procedure as that used to prepare **5a**: ^1H NMR (C_6D_6) δ 8.94 (d, 1, J = 6), 7.50 (dt, 2, Ph), 7.10−7.26 (m, 6, Ph), 7.00 (m, 2), 6.23 (s, 1, 2,4-Lut), 6.10 (sept, 1, OC*H*(CF$_3$)$_2$), 6.09 (d, 1, 2,4-Lut), 4.82 (sept, 1, J = 6.0, OC*H*(CF$_3$)$_2$), 2.39 (s, 3, 2,4-Lut), 1.87 (q, 6, AdN), 1.75 (br, 3, AdN), 1.49 (s, 3, 2,4-Lut), 1.3 (s, 6, AdN); ^{13}C NMR (C_6D_6) δ 310 (*C*Ph$_2$), 160.9, 153.0, 151.7, 151.2, 141.5, 129.5, 129.0, 128.6, 127.9, 127.38, 126.9, 123.2, 82.2 (O*C*H(CF$_3$)$_2$), 76.1 (═N*C*), 75.2 (O*C*H(CF$_3$)$_2$), 43.4 (NAd), 35.9 (NAd), 29.7 (NAd), 28.1 (Me, 2,4-Lut), 20.1 (Me, 2,4-Lut); ^{19}F NMR (C_6D6) δ 73.57 (1), 74.43 (2), 74.52 (1). Anal. Calcd for $MoC_{36}H_{36}N_2O_2F_{12}$: C, 50.71; H, 4.26; N, 3.28. Found: C, 50.65; H, 4.21; N, 3.31.

Synthesis of Mo(NAd)[C(Ph)C(Ph)CHCMe$_2$Ph][OCH(CF$_3$)$_2$]$_2$-(2,4-lutidine) (6). To a cold (−40 °C) ether solution (∼60 mL) of **2a** (645 mg, 0.79 mmol) was added diphenylacetylene (142 mg, 0.80 mmol). The resulting yellow mixture was stirred at room temperature for 6 h and then stripped of solvents in vacuum. The yellow solid residue obtained was recrystallized from a toluene/pentane mixture to afford **6** as a bright yellow microcrystalline solid; yield 530 mg (67%): ^1H NMR (C_6D_6) δ 8.75 (d, 1), 7.64 (d, 2), 6.80−7.40 (m, Ph's), 6.20 (m, 1, OC*H*(CF$_3$)$_2$), 6.16 (d, 1), 6.14 (2H, *m*-H and C*H*CMe$_2$Ph), 4.89 (m, 1, OCH(CF$_3$)$_2$), 2.30 (s, 3, *o*-Me), 1.76 (br, 6, CH$_2$'s), 1.64 (br, 3, CH's), 1.48 (br, 6, CH$_2$'s), 1.29 (s, 3, *p*-Me), 1.22 (3, 6, C*Me*$_2$-Ph); ^{13}C NMR (C_6D_6) δ 305.1, 160.4, 153.9, 150.9, 150.8, 149.4, 143.6, 140.8, 139.4, 130.1, 127.6, 127.5, 127.2, 127.0, 126.4, 125.8, 122.9, 83.9 (*C*Me$_2$Ph), 75.5 (NAd), 43.4 (NAd), 41.8 (*C*Me$_2$Ph), 35.7 (NAd, 29.8 (C*Me*$_2$Ph), 29.7 (C*Me*$_2$Ph), 29.4 (NAd), 27.8 (*o*-Me), 20.1 (*p*-Me); ^{19}F NMR (C_6D_6) δ −72.94, −73.20, −73.53, −73.95. Anal. Calcd for $MoC_{47}H_{48}N_2O_2F_{12}$: C, 56.63; H, 4.85; N, 2.81. Found: C, 56.58; H, 4.93; N, 2.58.

Synthesis of Mo(N-2,6-Me$_2$C$_6$H$_4$)(CHCMe$_2$Ph)(OC$_6$F$_5$)$_2$(quinuclidine) (7). Two equivalents of KOC_6F_5 was added to a cold solution (−40 °C) of 0.5 mol of [Mo(CHCMe$_2$Ph)(N-2,6-Me$_2$C$_6$H$_4$)(OSO$_2$CF$_3$)$_2$-(DME)] in 50 mL of THF. After 5 h at −40 °C, 1 equiv of quinuclidine was added and the reaction mixture was stirred for 2 h at room temperature. The solvents were evaporated in vacuo to give an orange powder. The orange powder was extracted with a minimum amount of toluene. The extract was filtered, and the solvents were removed from the filtrate in vacuo. The crude product was recrystallized from cold ether to give yields in the range 70−90%: ^1H NMR (C_6D_6) δ 14.16 (s, 1, C*H*CMe$_2$Ph *anti*, J_{CH} = 145 (from ^{13}C satellites)), 13.02 (s, 1, C*H*CMe$_2$Ph *syn*, J_{CH} = 115 (from ^{13}C satellites)), 7.12−6.75 (m, 8, aromatic), 2.93 (m, 6, NCH$_2$ *anti*), 2.75 (m, 6, NCH$_2$ *syn*), 2.72 (s, 6, N*Me*Ph *syn* and *anti*), 1.95 (s, 3, CHCMe*Me*′Ph), 1.73 (s, 3, CHCMe*Me*′Ph *syn*), 1.33 (s, 3, CHC*Me*Me′Ph *anti*), 1.10 (s, 3, CHC*Me*Me′Ph *syn*), 1.00 (m, 1, NCH$_2$CH$_2$C*H* *syn* and *anti*), 0.89 (m, 6, NCH$_2$C*H*$_2$ *syn* and *anti*); ^{13}C NMR δ 298.34 (*C*HCMe$_2$Ph *anti*), 298.17 (d, J = 117, *C*HCMe$_2$Ph *syn*), 155.51 (C$_{ipso}$ CMe$_2$*Ph anti*), 153.96 (C$_{ipso}$ CMe$_2$*Ph syn*), 148.6−136.48 (m, OC$_6$F$_5$), 135.50 (C$_o$ NAr), 128.67−125.75 (aromatics), 53.80 (N*C*H$_2$CH$_2$ *anti*), 53.27 (N*C*H$_2$CH$_2$ *syn*), 52.60 (*C*Me$_2$Ph *syn*), 51.47 (*C*Me$_2$Ph *anti*), 31.06 (C*Me*Ph *syn*), 30.86 (C*Me*Ph *anti*), 28.71 (C*Me*Ph *syn*), 27.90 (C*Me*Ph *anti*), 25.69 (NCH$_2$*C*H$_2$ *syn* and *anti*), 20.67 (N*Me*Ph *syn*), 19.62 (NCH$_2$CH$_2$C*H* *syn* and *anti*), 19.19 (N*Me*Ph *anti*). Anal. Calcd for $C_{37}H_{34}MoN_2F_{10}O_2$: C, 53.89; H, 4.16; N, 3.40. Found: C, 53.84; H, 4.27; N, 3.22.

Synthesis of Mo(N-2,6-*i*-Pr$_2$C$_6$H$_4$)(CHCMe$_2$Ph)[OCH(CF$_3$)$_2$]$_2$(2,4-lutidine) (8). This compound was synthesized in 74% yield by the same procedure as that used to prepare **2a**: ^1H NMR (C_6D_6) δ 13.80 (s, 1H, C*H*CMe$_2$Ph), 7.57 (d, 2H), 7.49 (d, 1H), 7.36 (t, 3H), 7.23 (t, 1H), 6.14 (s, 1H), 6.10 (d, 1H), 6.00 (m, 1H), 3.95 (m, 2H), 3.80 (m, 1H), 2.28 (s, 3H), 2.18 (s, 3H), 1.71 (s, 3H), 1.55 (s, 3H), 1.48 (d, 6H), 0.99 (d, 6H); ^{13}C NMR (C_6D_6) δ 295.9 (*C*Me$_2$Ph, J_{CH} = 127 Hz), 157.8, 156.3, 152.5, 151.0, 148.9, 147.8, 128.7, 17.8, 127.7, 126.5, 126.2, 123.82, 123.77, 77.4 (m, O*C*H(CF$_3$)$_2$), 75.6 (m, O*C*H(CF$_3$)$_2$), 54.6 (*C*Me$_2$Ph), 31.4 (Me), 29.1 (Me), 28.1 (*o*-Me), 24.2 (Me), 24.1 (Me), 22.5, 20.1 (Me); ^{19}F NMR (C_6D_6) δ −73.29, −73.88, −75.45, −75.68. Anal. Calcd for $MoC_{35}H_{40}N_2O_2F_{12}$: C, 49.77; H, 4.77; N, 3.32. Found: C, 49.91; H, 4.65; N, 3.10.

Photocatalyzed Isomerization of the Alkylidene Ligand in Mo(NAd)[C(*o*-TMS-C$_6$H$_4$)(CH═CHCHCMe$_2$Ph)][OCMe(CF$_3$)$_2$]$_2$ (3a/b). A sample of the equilibrium mixture of **3a/b** (71 mg, 0.078 mmol) and 6.8 μL of diphenylmethane (6.8 mg, 0.040 mmol) were dissolved in 0.80 mL of toluene-d_8. The deep red solution was then irradiated with a medium-pressure Hg lamp at −60 °C. The concentration of the minor component increased at the expense of the major product over a period of 24−48 h. The irradiated mixture was immediately transferred to a precooled NMR probe, and the disappearance of the minor product was followed by integration (TMS group).

Insertion Studies with Catalyst 2a. Bulk toluene-d_8 solutions of catalyst **2a** (64.7 mM) with Ph_2CH_2 (92.7 mM) as an internal standard and monomers PA (2.6 M), *o*-MePA (2.1 M), *o*-*i*-PrPA (2.9 M), *o*-*t*-BuPA (1.9 M) , and *o*-TMSPA (0.29 mL) were prepared. Typical insertion studies were carried out by adding monomer to the catalyst solution containing an internal standard (Ph_2CH_2). The catalyst concentration was measured by integration of the alkylidene resonance versus the CH_2 resonance of Ph_2CH_2. The amount of the α product was measured by the same method using the intensity of the H$_\beta$ and H$_\gamma$ resonances in the first insertion product, and the amount of the β addition product using the intensity of new alkylidene resonances.

Polymerization of *o*-TMSPA by 2a. Stock toluene solutions were prepared for both **2a** (13.9 mM) and the monomer *o*-TMSPA (0.23 M). The polymerization reactions were carried out under dinitrogen in a drybox by quick addition of the *o*-TMSPA solution to a vigorously stirred solution of **2a** at room temperature. In a typical experiment,

0.24 mL of the *o*-TMSPA solution (55.2 mmol) was quickly injected into a toluene solution of catalyst (50 mL bulk solution diluted to 3 mL). The solution turned purple within $^1/_2$ h, and the color did not change significantly thereafter. After 24 h, the reaction was brought into the air, and MeOH was quickly added to induce the precipitation of poly(*o*-TMSPA) as a dark purple solid. The polymer was collected by filtration, washed with MeOH, and dried in vacuo; yield 9.0 mg (93%). Polymers that had been exposed to air did not show any red-shifted absorption.

Reactions could also be quenched with 100 equiv of benzaldehyde or 8 equiv of acetic acid. Polymers prepared in the absence of air, which contained 20−30 equiv of *o*-TMSPA on the average, could be shown to isomerize to an air-sensitive form as described in the text.

Polymerization of *o*-TMSPA by 2c. A bulk toluene solution of *o*-TMSPA (0.40 M) was prepared. A typical polymerization was the following: Inside a drybox, catalyst **2c** (8 mg, 10 mmol) was dissolved in 10 mL of toluene; 1.00 mL of monomer solution (400 mmol) was quickly added to the solution. The polymerization solution turned to red and then purple within a few minutes at room temperature. After 3 h of stirring, ∼1.5 mL of polymerization solution was put into a separate vial and quenched with MeOH inside the drybox. The purple poly(*o*-TMSPA) precipitated out immediately as a powder and was collected by filtration, dried in vacuum, and used for GPC measurement. The same procedure was repeated after 22 h and 45 h stirring.

Kinetics Measurements of the Polymerization of *o*-TMSPA by 2a. Stock toluene solutions of the catalyst **2a** (10.3 mM) and *o*-TMSPA (0.41 M) containing internal standard Ph_2CH_2 (0.12 M) were prepared separately. Polymerization reactions were carried out by quick addition of toluene solutions of *o*-TMSPA and internal standard (Ph_2CH_2) to the toluene solutions of initiator **2a**, all of known concentration and volume, under pseudo-first-order conditions ([*o*-TMSPA]/[**2a**] = 80) inside a drybox. A typical kinetic run consisted of the following: 0.5 mL of catalyst solution was diluted with 3.50 mL of toluene. To this solution was quickly added 1.00 mL of monomer/internal standard solution with vigorous stirring. Aliquots of the polymerization solution (∼0.2 mL) were taken at intervals and quenched with an excess amount of MeOH (∼1.5 mL) immediately. The quenched reactions were filtered through Celite to remove the precipitated polymer. The filtrates were then analyzed by gas chromatography. The temperature inside the drybox (22 °C) was found to vary less than ±1 °C during polymerization experiments.

Four additional runs were carried out at $[\mathbf{2a}]_0 = 0.98$ mM with base added (Table 9b). In the run in which no base was added, it was assumed that [2,4-lutidine] = 0.98 mM (complete dissociation of lutidine). In the other runs [2,4-lutidine] was assumed to be the amount that had been added to the reaction. A plot of $[\mathbf{2a}]_0/k_{obs}$ versus [2,4-lutidine] gave $k_{2a} = 0.31\ s^{-1}\ M^{-1}$ and $K_{2a} = 61\ M^{-1}$ with $R^2 = 0.987$. Using $K_{2a} = 61\ M^{-1}$ the values for [2,4-lutidine] in Table 9b were recalculated and the plot was redone to give $k_{2a} = 0.32\ s^{-1}\ M^{-1}$ and $K_{2a} = 62\ M^{-1}$ with $R^2 = 0.996$ (Figure 4a).

Polymerization of *o*-MePA by 2a. Bulk toluene solutions of *o*-MePA (2.1 M) and catalyst 1 (12.3 mM) were prepared. A typical polymerization was the following. Inside a drybox, 0.24 mL of catalyst (3.0 mmol) solution was diluted to ∼5 mL. To this was quickly added 0.10 mL (210 mmol) of monomer solution. The solutions turned yellow, orange, and finally red within a few minutes at room temperature. After the solution was stirred for 24 h, methanol (∼15 mL) was added and the precipitated deep red poly(*o*-MePA) was collected by filtration and dried in vacuum overnight; weight 23 mg (95%).

Polymerization of *o*-*i*-PrPA by 2a. Bulk toluene solutions of *o*-*i*-PrPA (3.0 M) and catalyst 1 (7.5 mm) were prepared. Polymerization and polymer isolation were carried out as described for poly(*o*-MePA). A typical run with monomer (630 mmol) and catalyst (7.5 mmol) gave 87 mg (100%) polymer as a deep red solid.

Table 9. Observed Rate Constants for Polymerization of *o*-TMSPA by **2a** in Toluene (by GC) at 22 °C

(a) No Base Added

$[\mathbf{2a}]_0$ (mM)	k_{obs} ($\times 10^{-4}\ s^{-1}$)	$k_{obs}/[\mathbf{2a}]_0$ ($s^{-1}\ M^{-1}$)
0.41	1.48	0.36
0.52	2.08	0.25
0.72	2.10	0.29
0.98	3.00	0.31
1.03	3.85 (3.36)	0.26 (0.30)
1.42	4.26 (4.02)	0.30 (0.28)
1.89	6.41	0.34
2.06	6.66 (8.43)	0.31 (0.24)
2.46	7.71	0.31
2.51	7.50	0.30

(b) Base Added (Except Run 1)

$[\mathbf{2a}]_0$ (mM)	added [2,4-Lut] (mM)	adjusted [2,4-Lut]	k_{obs} ($\times 10^{-4}\ s^{-1}$)	$[\mathbf{2a}]_0/k_{obs}$ ($s^{-1}\ M^{-1}$)
0.98	0	0.93	3.00	3.27
0.98	4.53	5.28	2.31	4.24
0.98	8.74	9.36	1.93	5.08
0.98	12.8	13.3	1.76	5.57
0.98	16.9	17.3	1.50	6.53

Table 10. Observed Rate Constants for Polymerization of *o*-TMSPA by **7** in Toluene (by GC) at 22 °C with Base Added

$[\mathbf{7}]_0$ (mM)	[quinuclidine] (M)	k_{obs} ($\times 10^{-5}\ s^{-1}$)	$[\mathbf{7}]_0/k_{obs}$ ($s^{-1}\ M^{-1}$)
1.36	0.0122	1.77	77
1.36	0.0190	1.14	119
1.36	0.0272	0.78	174
1.36	0.0449	0.49	275

Polymerization of *o*-TMSPA by 7. Stock solutions of the monomer (1.05 M in toluene) and the catalyst (0.04 M in toluene) were prepared. The catalyst was added to 5 mL of toluene; 0.5 mL of the monomer solution was added rapidly to the stirred catalyst solution. The solutions turned immediately deep red and, after 3 h, purple. After 36 h, 10 equiv of benzaldehyde was added. After an additional 12 h, the purple solution was passed through alumina and the solvent was removed in vacuo, affording the polymer as a purple film (88−92 mg; 96−100%).

Kinetics Measurements of the Polymerization of *o*-TMSPA by 7. The general procedure was the same as in the polymerization using **2a** as the initiator. The results are shown in Table 10.

Acknowledgment. R.R.S. thanks the Director, Office of Basic Energy Research, Office of Basic Energy Sciences, Chemical Sciences Division of the U.S. Department of Energy (Contract DE-FG02-86ER13564), for support.

Supporting Information Available: Detailed description of X-ray data collection, structure solution, and refinement, labeled ORTEP diagrams, and tables of fractional coordinates and anisotropic thermal parameters for **1a** and **2a** (24 pages). This material is contained in many libraries on microfiche, immediately follows this article in the microfilm version of the journal, can be ordered from the ACS, and can be downloaded from the Internet; see any current masthead page for ordering information and Internet access instructions.

JA954155W